



OPEN Elaboration of newly synthesized tetrahydrobenzo[*b*]thiophene derivatives and exploring their antioxidant evaluation, molecular docking, and DFT studies

Mina G. Balamon✉, Ashraf A. Hamed, Eman A. El-Bordany, Ahmed E. Swilem & Naglaa F. H. Mahmoud

Herein, 2-amino-6-(tert-butyl)-4,5,6,7-tetrahydrobenzo[*b*]thiophene-3-carbonitrile (**1**) was synthesized in excellent yield through gewald reaction in multi components one pot reaction. Compound **1** was utilized as a building block to synthesize a new group of tetrahydro benzo[*b*] thiophene congeners. The chemical structure of all the novel tetrahydro benzo[*b*]thiophene derivatives were elucidated through the melting point, elemental analysis, FT-IR, ¹H-NMR, and mass spectroscopy. Furthermore, the total antioxidant capacity (TAC) of all the newly synthesized heterocyclic derivatives was evaluated according to the phosphomolybdenum method using ascorbic acid as standard. The findings revealed that compounds **1**, **16**, and **17** demonstrated significant antioxidant potency comparable to that of ascorbic acid. This suggests the potential of these heterocycles as promising candidates for antioxidant drugs in the treatment of oxidative stress-related diseases. Finally, molecular docking was conducted to study the binding affinity for the most potent antioxidant compounds **1**, **16**, **17** and ascorbic acid inside the interactions of compounds **1**, **16**, and **17** with the Keap1 (Kelch-like ECH-associated protein 1) protein (PDB: 7C5E), compared to the co-crystallized ligand triethylene glycol (PGE) and ascorbic acid as a reference drug for antioxidants. DFT calculations and global descriptors were calculated for the most potent compounds to correlate the relation between chemical structure and reactivity.

Keywords Antioxidant, Docking, DFT, 2-amino thiophene-3-carbonitrile

From medicinal chemistry to material science, S-heterocyclic cores, particularly those based on thiophene, are recognized for their paramount significance in diverse domains, including pharmaceuticals¹, dyes², and agrochemicals³. There are a wide range of biologically active products⁴, many of which demonstrate antifungal activity⁵, anticancer activity toward the six cancer cell lines (A549, H460, HT-29, MKN-45, U87MG, and SMMC)⁶, anti-inflammatory⁷, antioxidant⁸, antitumor⁹, antitubercular¹⁰ as demonstrated in (Fig. 1), anticoagulant and antithrombotic activities¹¹. The 2-Amino thiophene derivatives stand out as crucial intermediates in organic synthesis, giving rise to diverse heterocyclic systems with useful applications^{12,13}. For The synthesis of thiophen-2-amines, involving the challenging introduction of an amino group into an existing thiophene moiety, has garnered attention in organic chemistry. Numerous methodologies for synthesizing 2-aminothiophenes have been reported over the past three decades, with a focus on their applications in pharmaceuticals, agriculture, pesticides, and dyes. A series of reviews have been published dealing with the latest accomplishments of 2-aminothiophenes¹⁴. Gewald's versatile, synthetic method developed by him has brought much attention to the chemistry of 2-aminothiophenes due to the convenience of availability¹⁵. Gewald method was known as the most well-established approach for preparing 2-amino thiophenes, relies on a three-component reaction involving an α -ketone, an activated nitrile, and elemental sulfur in the presence of a basic catalyst¹⁶⁻¹⁹.

The core structure is formed in the multi-component reaction between α -ketone or an aldehyde, an activated nitrile, and sulfur. This method has been universally adopted for the synthesis of substituted 2-amino thiophenes, since its introduction in 1961, But still, the research and generation of new compounds with this method is

Department of Chemistry, Faculty of Science, Ain Shams University, Cairo 11566, Egypt. ✉email: minagirgis@sci.asu.edu.eg

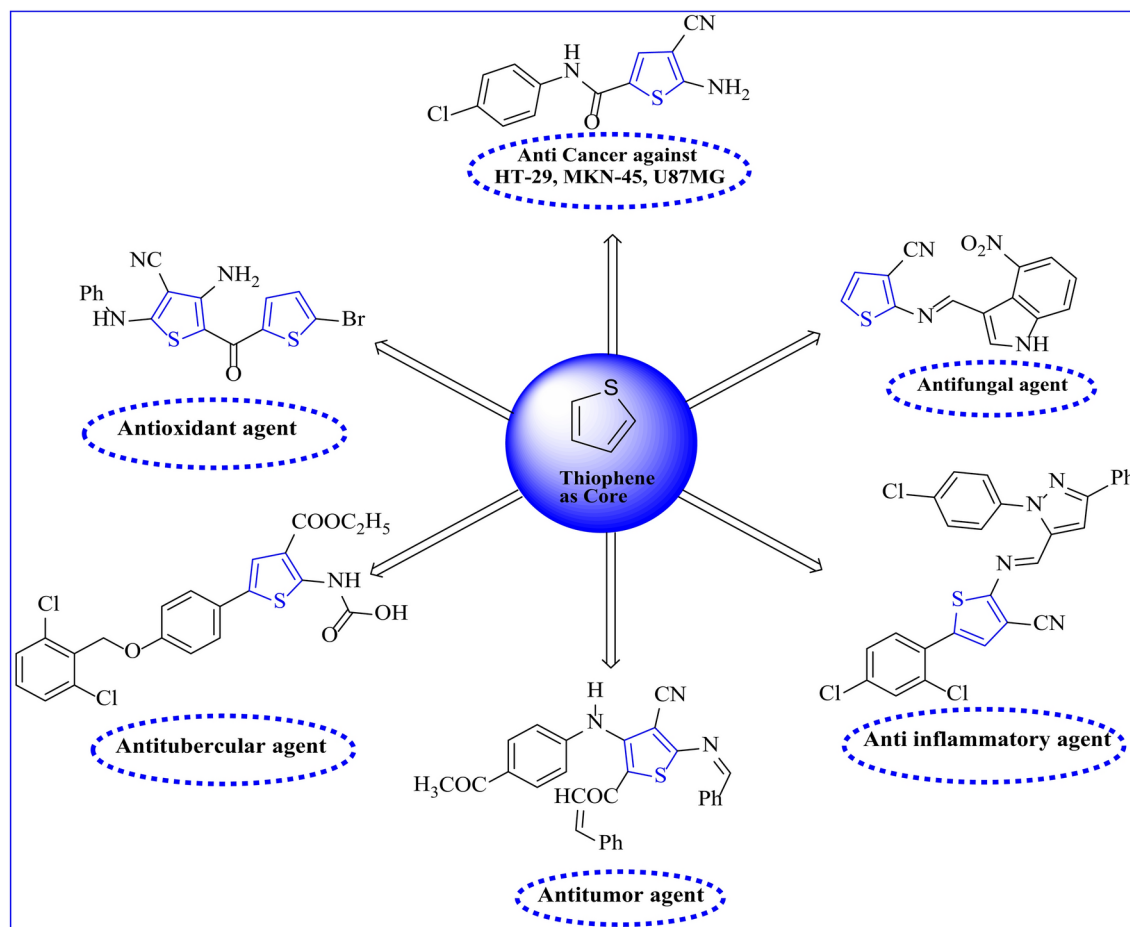


Fig. 1. Various biological activities based on thiophene ring.

rapidly expanding due to its easy adaptability in the field of pharmaceutical and material chemistry. While the one-pot Gewald synthesis is widely accepted, a step-wise procedure involving the preparation of α,β -unsaturated nitrile through the condensation of α -ketone or aldehyde with an activated nitrile, followed by a base-promoted reaction with sulfur, promises a more comprehensive understanding of the reaction mechanism^{14,15,20}. Notably, among thiophene derivatives, 2-amino thiophenes emerge as versatile materials with applications spanning various scientific disciplines. They play pivotal roles in exhibiting potent biological activities, such as serving as allosteric enhancers of adenosine receptors²¹ and glucagon receptor antagonists²². Additionally, their applications extend to materials science, including usage in dyes²³, conductivity-based sensors²⁴, and bio-diagnostics^{15,25}.

Additionally, Tetrahydrobenzo[*b*]thiophene derivatives display a range of biological activities, notably significant anti-inflammatory properties²⁶. Also, the compounds **I**, **II**, **III**, and **IV** which containing benzo[*b*]thiophene nucleus exhibit potent antioxidant activity^{27,28} as shown in (Fig. 2), demonstrating the capability to inhibit free radical-induced lipid oxidation and the formation of lipid peroxides, with inhibition rates ranging from approximately 19 to 30%²⁷.

As depicted in Fig. 3, tetrahydrobenzo[*b*]thiophene derivative **IX** and tetrahydrohepta[*b*]thiophene derivative **X** are recognized as significant fused thiophene derivatives, demonstrating potent antioxidant activities^{29,30}. Based on the structural features of the **IX** and **X**, and as an extension of our previous research on the design of new heterocyclic pharmacophores^{31–44}. Herein, we describe the design rationale of the target compounds, synthesis of a new group of tetrahydrobenzo[*b*]thiophene congeners, and in vitro antioxidant evaluation according to the phosphomolybdenum method using ascorbic acid as standard. A variety of analytical techniques, such as elemental analysis, ¹HNMR, IR, and mass spectroscopy, were employed to elucidate the structures of these new heterocyclic derivatives. The total antioxidant capacity (TAC) assay was employed to assess the synthesized compounds' ability to combat oxidative stress. Additionally, the study delved into the structure–activity relationship (SAR) and explored potential mechanisms of action for these derivatives.

Results and discussion

Chemistry

The thiophene ring incorporating an enaminonitrile functional group, specifically 2-amino-6-(tert-butyl)-4,5,6,7-tetrahydrobenzo[*b*]thiophene-3-carbonitrile **1**, was synthesized via the Gewald reaction in a one-pot procedure. This involved heating a mixture of malononitrile, *p*-*t*-butyl cyclohexanone, and elemental sulfur

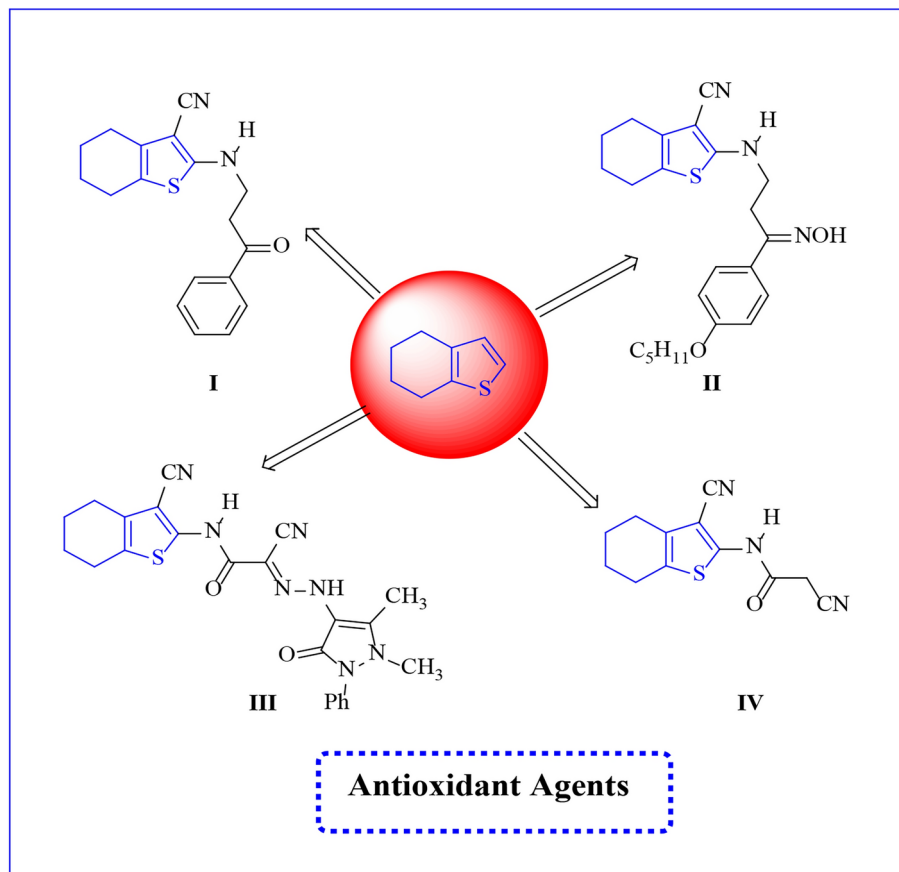


Fig. 2. Some reported tetrahydro benzo[*b*]thiophene derivatives such as antioxidant.

in absolute ethanol containing a catalytic amount of triethyl amine. The initial compound **1** was obtained through a sequential process, starting with the preparation of α,β -unsaturated nitrile through the condensation of α -ketone with malononitrile **1'**, followed by a base-promoted reaction with sulfur (Scheme 1). Compound **1** was previously prepared according to the literature procedure with different conditions and techniques⁴⁵. The FT-IR spectrum of compound **1** showed a strong absorption band at $\nu = 3323\text{--}3428\text{ cm}^{-1}$ corresponding to the amino group and band at $\nu = 2201\text{ cm}^{-1}$ for cyano group. Moreover, the ¹H-NMR spectra showed $\delta = 0.89$ ppm for *t*-butyl group and D₂O-exchangeable broad singlet peak due to the amino group at $\delta = 6.93$. A plausible mechanism for the formation of compound **1** is the Michael addition of the active methylene of malononitrile on the α -ketone, followed by nucleophilic attack of active methylene of cyclohexanone on sulfur lattice, and then intramolecular nucleophilic attack as shown in (Scheme 2).

In this study, compound **1** served as a foundational element for generating a variety of heterocyclic frameworks containing NSO heteroatoms. The combination of compound **1** with formamide and/or formic acid resulted in the production of the respective pyrimidine derivatives, namely **2** and **3** (Scheme 3). These compounds had been synthesized earlier following a method outlined in the literature⁴⁶. The FT-IR spectrum of compound **2** indicated the absence of the CN absorption band, replaced by an absorption band at $\nu = 3313\text{--}3424\text{ cm}^{-1}$ attributed to NH₂ stretching. Additionally, its ¹H-NMR spectrum exhibited a D₂O-exchangeable singlet peak at $\delta = 4.61$ ppm, corresponding to the NH₂ group in the pyrimidine ring, and a singlet peak at $\delta = 8.32$ ppm for the pyrimidine CH proton.

On the other hand, the FT-IR spectrum of compound **3** showcased an absorption band at $\nu = 1658\text{ cm}^{-1}$, attributed to the C=O in the pyrimidinone ring, along with a newly appearing absorption band at $\nu = 3157\text{ cm}^{-1}$ due to NH stretching. The ¹H-NMR spectrum of compound **3** revealed a singlet peak at $\delta = 7.98$ ppm for the pyrimidine CH proton and a D₂O-exchangeable singlet peak at $\delta = 12.29$ ppm corresponding to the NH group in the pyrimidine ring.

Also, Compound **1** underwent reactions with phenyl isothiocyanate and carbon disulfide, resulting in the formation of the thiophen-2-yl thiourea derivative **4** and the thieno[2,3-*d*]pyrimidine-2,4(1*H*,3*H*)-dithione derivative **5**, respectively (Scheme 3). The FT-IR-spectrum of compound **4** showed the appearance of an absorption band at $\nu = 3208$ and 3288 cm^{-1} due to 2NH stretching, and a band at $\nu = 2205\text{ cm}^{-1}$ due to the cyano group. In addition, the ¹H-NMR analysis indicated a D₂O-exchangeable singlet peak at $\delta = 8.12$ ppm and $\delta = 8.19$ ppm due to the 2NH. However, the FT-IR-spectrum of compound **5** showed the lack of an absorption band for the cyano group and the existence of absorption bands at $\nu = 3108$ and 3379 cm^{-1} due to the 2NH of

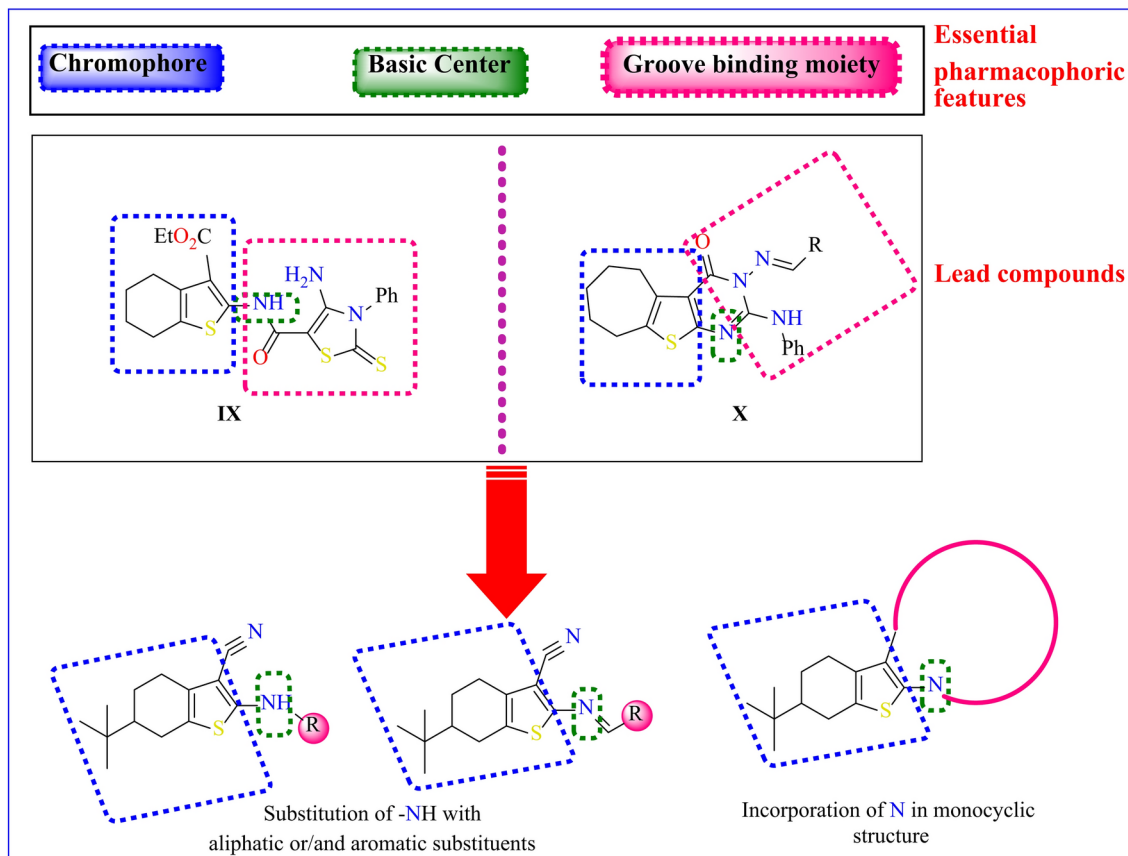
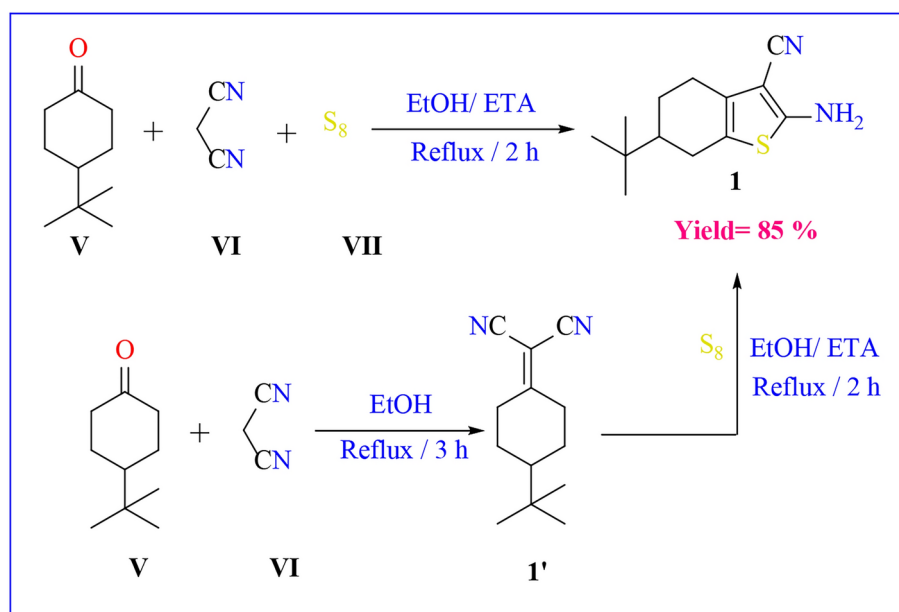
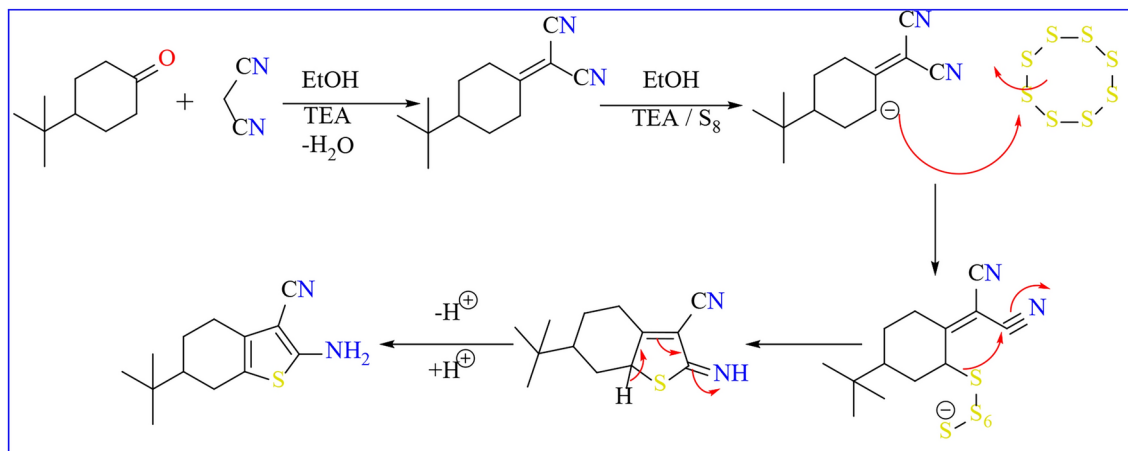


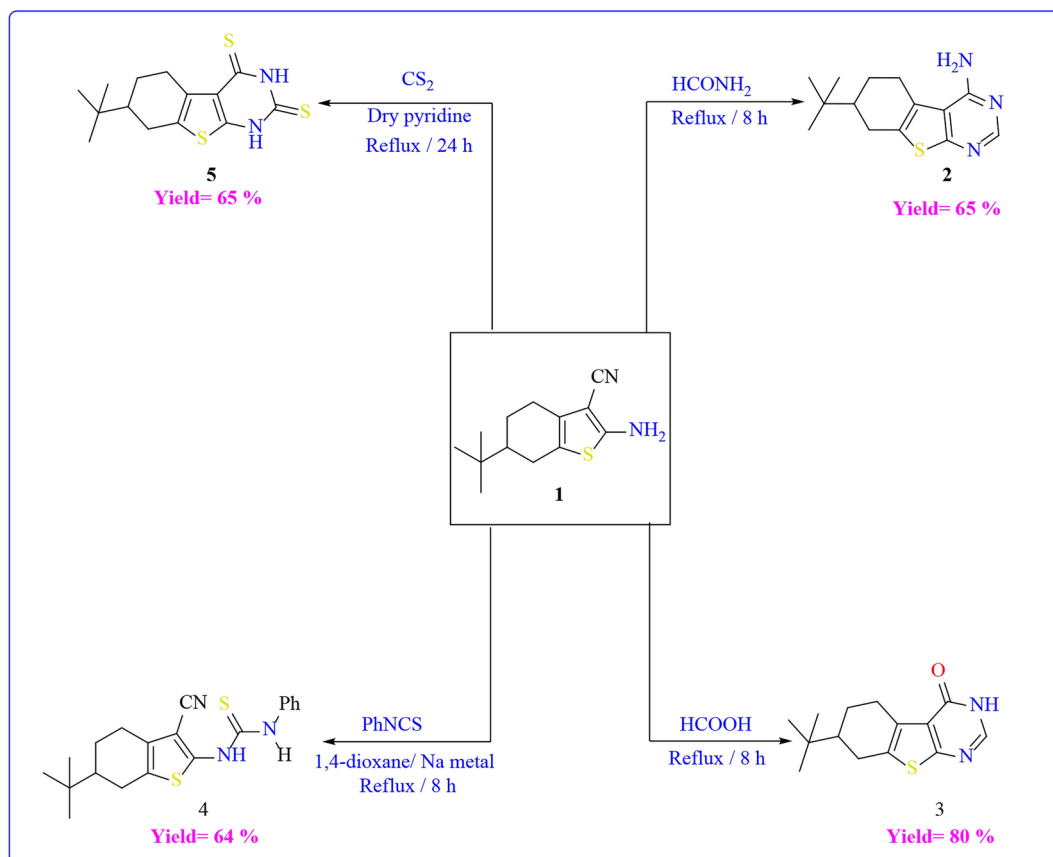
Fig. 3. The suggested design rationale of the target candidates 2–21 based on tetrahydro benzo[*b*]thiophene moiety.



Scheme 1. One pot and multi steps Synthesis of starting material.



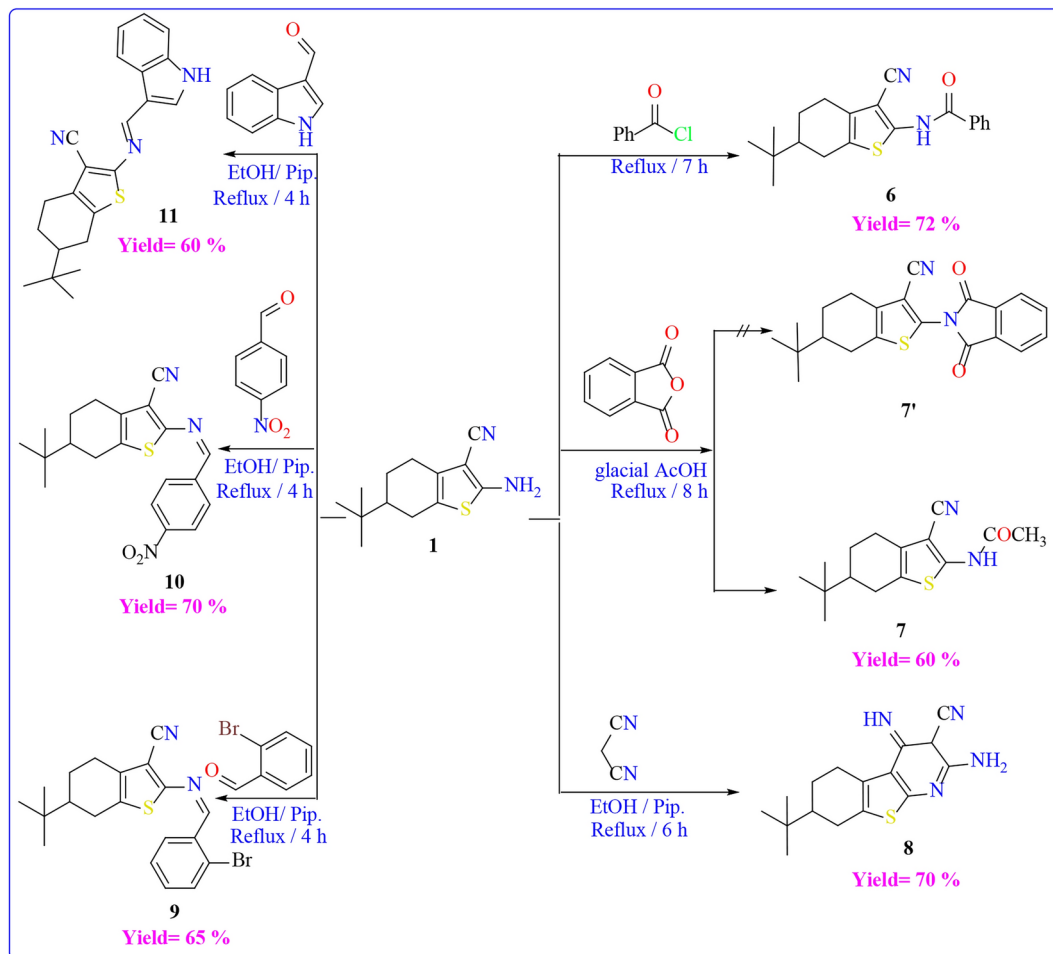
Scheme 2. Mechanistic illustration for the formation of compound **1**.



Scheme 3. Reactions of compound **1** with different electrophile reagents.

the pyrimidine ring. Its $^1\text{H-NMR}$ spectrum exhibited a D_2O -exchangeable singlet peak at $\delta = 12.29$ ppm and $\delta = 13.23$ ppm due to the 2NH.

In contrast to this, compound **1** was allowed to react with different electrophilic reagents as outlined in (Scheme 4). First, The acylation of compound **1**, achieved by treating it with benzoyl chloride, resulted in the formation of the corresponding *N*-(3-cyanothiophen-2-yl)benzamide **6**. The FT-IR spectrum of compound **6** confirmed the emergence of an absorption band at $\nu = 1667\text{ cm}^{-1}$ due to the carbonyl group of benzamide. In addition, the $^1\text{H NMR}$ showed multiplet peaks at range $\delta = 7.55\text{--}7.96$ ppm due to the aromatic CH proton, and D_2O -exchangeable singlet peak at $\delta = 11.70$ ppm due to the NH. Upon the reaction of compound **1** with phthalic anhydride in glacial acetic acid, the formation of two potential products was anticipated. However, both elemental analysis and spectral data confirmed the structure of **7** and ruled out the formation of structure



Scheme 4. Reactions of compound **1** with different electrophile reagents.

7' due to the absence of CH aromatic in ^1H NMR spectrum. The FT-IR spectrum of compound **7** exhibited the existence of an absorption band at $\nu = 1697\text{ cm}^{-1}$ due to the carbonyl group. Its ^1H NMR indicated a singlet peak at $\delta = 2.16$ ppm due to the methyl group, and a D_2O -exchangeable singlet peak at $\delta = 11.49$ ppm due to the NH. The thieno[2,3-*b*]pyridine-5-carbonitrile derivative **8** was synthesized by subjecting starting material **1** to reflux conditions with malononitrile in absolute ethanol, featuring a catalytic amount of piperidine. The mass spectrum of compound **8** showed its molecular ion peak at $m/z = 300$ (M^+). Moreover, its ^1H NMR spectrum indicated a singlet peak at $\delta = 2.17$ ppm due to pyridine CH proton, D_2O -exchangeable singlet peak at $\delta = 6.92$ and $\delta = 11.50$ ppm due to the amino group and the NH group respectively.

Moreover, Compound **1** underwent condensation with *o*-bromo benzaldehyde, *p*-nitro benzaldehyde, and indole-3-carboxaldehyde in an ethanolic solution under reflux conditions, resulting in the formation of the respective Schiff's bases **9**, **10**, and **11** respectively, as shown in (Scheme 7). The structures of the synthesized compounds were determined through spectroscopic and elemental analyses. The absence of the characteristic band of the amino group was observed in the FT-IR spectrum of the compounds. Additionally, the FT-IR spectrum of compound **11** exhibited bands at $\nu = 3328\text{ cm}^{-1}$, indicating the presence of NH groups. The ^1H -NMR analysis of the synthesized compounds **9**, **10**, and **11** revealed the presence of aromatic CH protons within the range of $\delta = 7.23$ – 8.40 ppm, in addition to compound **11** its ^1H -NMR showed a singlet peak at $\delta = 8.71$ ppm due CH proton of pyrrole ring and D_2O -exchangeable singlet peak at $\delta = 12.09$ ppm corresponding to the NH group.

Furthermore, the amino group in compound **1** akin to a primary aromatic amine, demonstrating the ability to produce the corresponding diazonium salt when exposed to nitrous acid within a temperature range of 0 to 5°C . Additionally, it can engage in coupling reactions with various nucleophilic reagents, including ethyl cyanoacetate and/or ethyl acetoacetate to afford the corresponding coupling products **13** and **14** respectively (Scheme 5). The structures of the synthesized compounds were determined through spectroscopic and elemental analyses. The FT-IR spectrum of compounds **13**, and **14** revealed characteristic bands at $\nu = 3424$ and 3363 cm^{-1} indicating the presence of NH groups respectively. Also appeared absorption bands at $\nu = 1732$ and 1740 cm^{-1} respectively due to the carbonyl groups of esters. The mass spectrum of compounds **13** and **14** showed their molecular ion peak (M^+) at $m/z = 358$ and 375 respectively.

The creation of aceto hydrazide derivative **15** was facilitated through the reaction of compound **13** with hydrazine hydrate in absolute ethanol. The structural validation was achieved via spectral analysis. The FT-IR

displayed a lack of the characteristic absorption band for the carbonyl ester and the existence of the NH₂ and NH groups at a range of $\nu = 3198\text{--}3314\text{ cm}^{-1}$. Its ¹H-NMR exhibited that D₂O-exchangeable singlet peak at $\delta = 5.42$, 7.64, and 12.41 ppm due to the amino group and the two NH groups respectively.

Compound **3**, specifically the thieno[2,3-d]pyrimidine-4(3H)-one derivative, served as a valuable key intermediate for the subsequent synthesis of novel pyrimidin-thione derivatives. Firstly, it underwent treatment with phosphorous pentasulfide in dry toluene, yielding the corresponding pyrimidine-4(3H)-thione derivative **16** in only one step. On the other hand, compound **16** has been previously prepared in literature⁴⁶ on two steps by reaction of pyrimidinone **3** with POCl₃/PCl₅ followed by reaction the product with thiourea. The FT-IR spectrum of **16** revealed the absence of the carbonyl group of pyrimidinone and the presence of an absorption band at $\nu = 1362\text{ cm}^{-1}$ corresponding to the C=S group. Meanwhile, its mass spectrum exhibited a peak at $m/z = 278\text{ (M}^+)$. Subsequently, compound **16** underwent reactions with hydrazine hydrate and ethyl chloroacetate, resulting in the formation of 4-hydrazinylthieno[2,3-d]pyrimidine derivative **17** and ethyl 2-(thieno[2,3-d]pyrimidin-4-ylthio)acetate derivative **18** respectively, as illustrated in (Scheme 6). The FT-IR spectrum of compound **17** showed the bands at $\nu = 3196$ and $3313\text{--}3392\text{ cm}^{-1}$, indicating the presence of NH and NH₂ groups. In addition, the ¹H-NMR analysis indicated a D₂O-exchangeable singlet peak at $\delta = 4.61$ ppm and $\delta = 7.88$ ppm due to the NH₂ and NH group respectively. The FT-IR spectrum of compound **18** revealed absorption bands at $\nu = 1746\text{ cm}^{-1}$ corresponding to the stretching vibrations of the C=O ester group. Its ¹H-NMR analysis exhibited a triplet peak at a range $\delta = 1.17\text{--}1.21$ ppm for CH₃ and multiplet peak at a range $\delta = 4.10\text{--}4.16$ ppm due to $\text{CH}_2\text{-S}$, and CH₂ of ester.

Additionally, the synthesis of compound **19** is achievable by subjecting compound **1** to hydrolysis in 70% sulfuric acid under reflux on a water bath. An alternative method involves preparing it through the reaction of *p*-*t*-butyl cyclohexanone with cyano acetamide and a sulfur element in the presence of triethyl amine, as outlined in (Scheme 7). The FT-IR spectrum of compound **19** displayed the absence of the cyano group and the appearance of absorption bands at a range of $\nu = 3322\text{--}3497\text{ cm}^{-1}$, indicating the presence of two amino groups. In addition, the ¹H-NMR analysis indicated a D₂O-exchangeable singlet peak at $\delta = 7.19$ ppm and $\delta = 7.88$ ppm due to the 2NH₂ groups.

Treating derivative **19** of 2-aminothiophene-3-carboxamide with formic acid yielded the same product obtained from the reaction of compound **1** with formic acid under reflux conditions (refer to Scheme 7). Subsequently, derivative **19** underwent condensation with *p*-nitrobenzaldehyde, benzoyl chloride, and ethyl chloroacetate, resulting in the formation of Schiff base product **20**, pyrimidin-4(3H)-one derivative **21**, and pyrimidine-2,4(1H,3H)-dione derivative **22** (as depicted in Scheme 8). The identification of the structures of these compounds was confirmed through spectroscopic and elemental analysis. Notably, the FT-IR spectrum of compound **20** exhibited an absence of absorption bands indicative of amino groups. Additionally, its mass spectrum displayed a molecular ion peak at $m/z = 518$. The FT-IR spectra of compounds **21** and **22** revealed distinctive absorption bands corresponding to carbonyl groups at $\nu = 1679$ and 1657 cm^{-1} , and NH groups within the range of $\nu = 3169\text{--}3207\text{ cm}^{-1}$, respectively. In the ¹H-NMR analysis of compound **21**, a D₂O-exchangeable singlet peak at $\delta = 12.99$ ppm was observed, attributed to the NH group. Similarly, the ¹H-NMR spectrum of compound **22** displayed a D₂O-exchangeable singlet peak at $\delta = 11.32$, and $= 12.24$ ppm for the 2NH groups.

Antioxidant activity

Determination of total antioxidant capacity (TAC)

The synthesized heterocyclic compounds **1–21** were evaluated for their *in vitro* antioxidant activity. The results of this antioxidant activity were compared with those of ascorbic acid, which was used as a standard reference drug. Compounds **1**, **16**, and **17** displayed high antioxidant properties, comparable to that of ascorbic acid. Meanwhile, Compounds **2**, **7**, **9**, **10**, **11**, **15**, **18**, **19**, **20** and **21** reported moderate antioxidant activities. This suggests the presence of free amino and NH groups in compounds **1**, **16**, and **17** respectively. Which enhances the antioxidant activity by increasing their hydrogen donor capacity^{47,48}. Also, it can be concluded that compounds **1**, **2**, **7**, **9**, **10**, **11**, **15**, **16**, **17**, **18**, **19**, **20** and **21** have potent to moderate antioxidant activity in comparison with ascorbic acid, which might be beneficial to develop new therapeutic agents for the treatment of oxidative stress-associated diseases.

Docking study

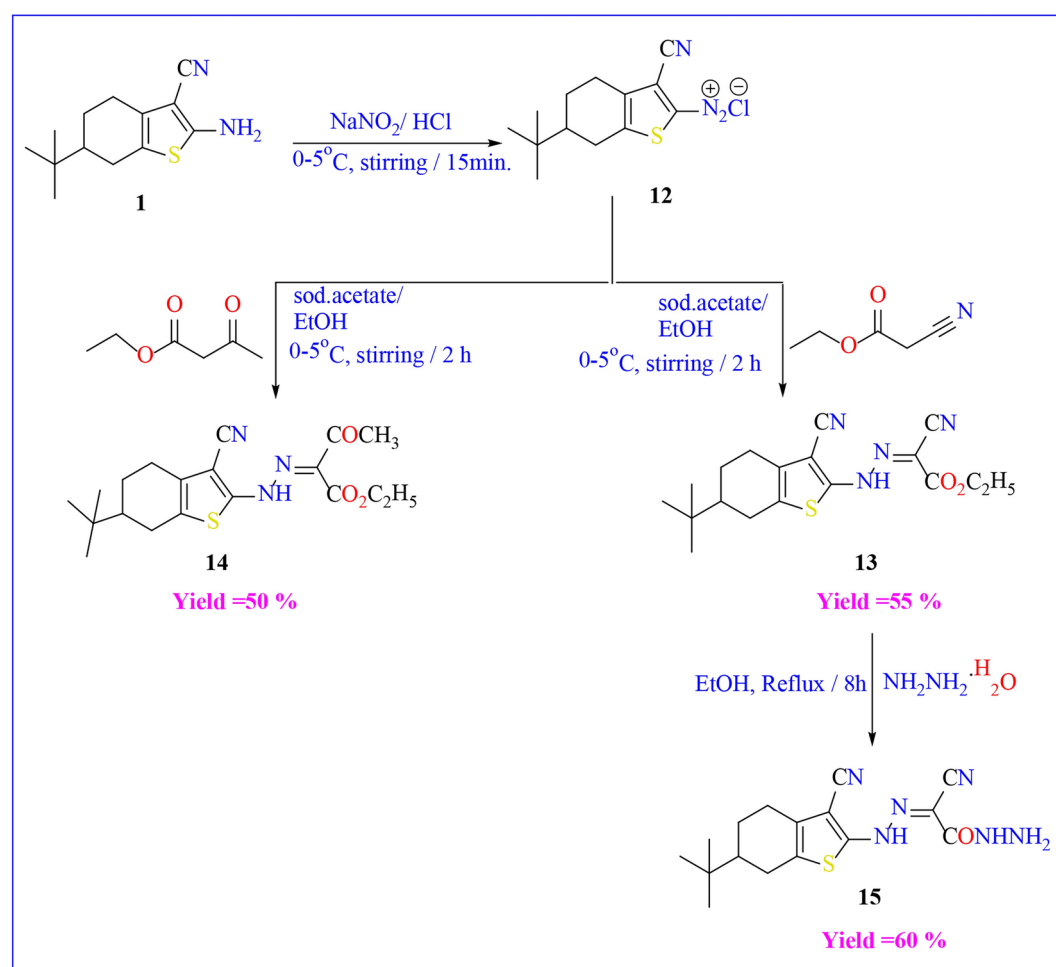
Molecular docking serves as a prevalent computational technique extensively applied in molecular biology and drug discovery. It is utilized to anticipate how a small molecule ligand binds to a protein receptor. The primary objective of this method is to pinpoint the most energetically advantageous alignment and positioning of the ligand within the receptor's binding site. This process is vital for understanding the interactions between a ligand and its receptor, which is essential for developing new drugs and designing effective drug therapies by combining structural and computational approaches^{48,49}. Furthermore, Kelch-like ECH-associated protein 1 (Keap1) is a therapeutic target for conditions linked to oxidative stress and inflammation. Currently, there are three covalent Keap1-binding drugs available; however, noncovalent inhibitors that disrupt the Keap1 interaction with nuclear factor erythroid 2-related factor 2 (Nrf2) present a promising alternative approach. Both types of inhibitors function by preventing the degradation of Nrf2, which subsequently induces the expression of antioxidant and anti-inflammatory proteins⁵⁰. So, we evaluated the interactions of compounds **1**, **16**, and **17** with the Keap1 (Kelch-like ECH-associated protein 1) protein (PDB: 7C5E), compared to the co-crystallized ligand triethylene glycol (PGE) and ascorbic acid as a reference drug for antioxidants. The docking study of the synthesized compounds was performed with Keap1 to predict if these compounds bind with Keap1 to activate Nrf2. Previously, it has been reported that the inhibition of Keap1 is a strategy that can lead to the activation of Nrf2 (nuclear factor erythroid 2-related factor 2), resulting in increased expression of antioxidant and detoxification genes. Therefore, inhibiting Keap1 activates the Nrf2-mediated antioxidant response, leading to increased

expression of genes that protect cells from oxidative stress and promote cellular survival. This pathway is a promising target for therapeutic interventions aimed at enhancing cellular defense mechanisms⁵¹. The binding free energies (ΔG) of synthesized candidates, ascorbic acid, and the co-crystallized ligand (PGE) in comparison to Keap1 have been summarized in (Table 1).

A re-docking validation step was successfully carried out to guarantee the precision of the docking procedure. The most active candidates (**1**, **16**, and **17**) were submitted to a docking process into the Keap1 (7C5E) sites to better understand the pattern by which the studied compounds bonded to the active site. According to the docking score values and binding mode, the affinities of the most potent newly synthesized ligands (**1**, **16** and **17**) and ascorbic acid towards the target proteins were contrasted (Table 1) showed that ascorbic acid gives a binding score of -5.21 kcal/mol while compounds **1**, **16** and **17** have a higher binding affinity than ascorbic acid with binding free energy -6.04 , -6.48 and -6.94 kcal/mol respectively. The analysis of 2D and 3D interaction figures (Table 2) reveals that compounds **1**, **16**, and **17** exhibit binding with the Keap1 protein at the same site as the co-crystallized ligand (PGE) with different interactions. However, these compounds display distinct interactions. Specifically, the thiophene ring of compounds **16**, and **17** interacts with Keap1 protein by Pi-H bond with ILE 559 amino acid. Additionally, the amino group of compound **1** binds with the same amino acid ILE 559 by an H-donor bond. Notably, this amino group is the site to which the OH group of the co-crystallized ligand (PGE) binds. This observation helps elucidate the heightened reactivity of the synthesized compound compared to ascorbic acid, as detailed in (Table 1).

DFT calculations

The chemical and biological characteristics of molecules are fundamentally understood by theoretical DFT calculations⁵². Within DFT, electron density plays a crucial part in determining the chemical reactivity features and holds information about the molecular properties. To comprehend the reactivity and selectivity at a specific atomic site inside a molecule, several DFT-based local reactivity descriptors using electron density were proposed^{53,54}. As a result, theoretical computations yield a large number of quanta chemical parameters. The critical chemical activities of the molecules are explained by the computed parameters. Molecule calculations are performed by numerous programs. Gaussian09 RevD.01 and Gauss View 6.0 are these programs^{55,56}. Moreover, the global reactivity descriptors can be obtained using the energies of LUMO & HOMO for the most potent

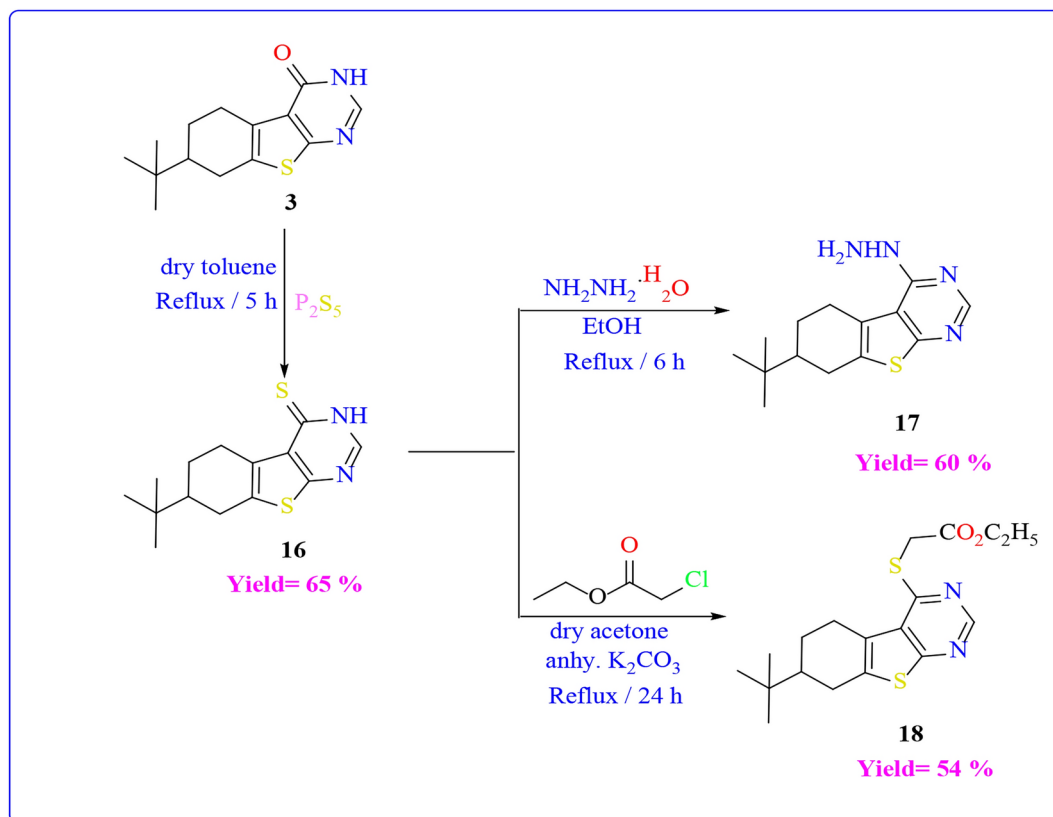


Scheme 5. Reactions of diazonium salt of compound **1** with active methylene.

antioxidant synthesized thiophene moiety **1**, **16**, **17** were determined by DFT using the B3LYP method along at the 6–31 G (d, p) basis sets⁵⁷ and tabulated in (Table 3).

Furthermore, it has been demonstrated that The Ionization potential (I), Electron affinity (A), Electronegativity (χ), Chemical potential (P), Chemical hardness(η), and Chemical softness (S) are excellent descriptors of biological activity and are thought to be indications of global reactivity³⁶. A compound's chemical stability is largely determined by its energy gap (the difference between its HOMO and LUMO states). Compounds with smaller energy gaps are thought to be more stable, and more likely to donate electrons (HOMO) or accept electrons (LUMO) that making it a potentially effective antioxidant, with lower redox potential which indicates a higher tendency to undergo oxidation or reduction reactions and can readily undergo electronic transitions While this is desirable for antioxidants that need to participate in redox reactions. According to the results listed in Table 3 and shown in (Fig. 4), compound **16** > **1** > **17** > ascorbic acid in an antioxidant activity where compounds **16** and **1** are close in their value of ΔE and all produced compounds have an energy gap smaller than that of ascorbic acid. The activity and Convergence in values for compound **1** and **13** is consistent with the experimental results listed in (Table 4).

Moreover, the ionization potential (I) is a crucial parameter for understanding the redox properties and antioxidant potential of a molecule. A lower ionization potential generally indicates a molecule's enhanced ability to donate electrons, making it more effective in combating oxidative stress. Analyzing the ionization potential, along with other parameters like the HOMO–LUMO gap, provides a comprehensive picture of the electron transfer capabilities of antioxidants. Based on the value of the ionization potential listed in Table 3, it was shown that compound **1** < **16** < **17** in ionization potential and this means that compound **1** > **16** > **17** as antioxidant and this is completely consistent with the practical results in Table 4. In the context of studying antioxidants, chemical softness (S) and chemical hardness (η) can offer valuable insights into the molecule's response to changes in its environment and its potential as a reactive species scavenger. Values reflect the polarization of the molecule; a higher softness value is more polarizable than the hard one and exhibits higher chemical reactivity due to its lower energy requirement for the excitation process. Consequently, the chemical softness of compounds **1**, **16**, and **17** in Table 3 reflects their elevated chemical softness than ascorbic acid, rendering them more polarized. A reciprocal correlation exists between the chemical potential (μ) and electronegativity (χ) concerning their influence on electron donation capability. As the chemical potential rises and electronegativity declines, there is an augmentation in the compound's capacity to donate electrons. The analysis of (μ) and (χ) reveals that compound **1** displays lower electronegativity and greater electron-donating potential than compounds **16** and **17** Which is proven practically in (Table 4).



Scheme 6. The reactions of compound **16** with various reagents.

Fukui function

One significant theoretical framework for determining the features of quantum chemistry is provided by density functional theory, or DFT^{58,59}. Within DFT, the electron density plays a crucial part in determining the chemical reactivity features and holds information about the molecular properties. To comprehend the reactivity and selectivity at a specific atomic site inside a molecule, several DFT-based local reactivity descriptors including electron density were presented^{53,54}. Numerous studies have revealed that Fukui functions^{60–64} are an effective intramolecular reactivity descriptor. They represent the local reactivity of the studied compounds. It is considered that the condensed Fukui functions can give relevant information regarding the reactive sites and the type of biochemical reaction in which they participate. For reactions with radicals' reaction site indices, Fukui function f_k^0 is proposed. This function governing radical attack and given by⁶⁵:

$$f_k^0 = [q_k(N+1) - q_k(N-1)]/2.$$

where:

$q_k(N+1)$: electronic population of k atom in an anionic molecule.

$q_k(N-1)$: electronic population of k atom in a cationic molecule.

In the present study, the values of Fukui function were calculated. If $f_k^0 > 0$, then the site is prone to radical attack. The positive values of Fukui function were collected and tabulated in (Table 5).

The calculated f_k^0 values predict that the possible sites for the radical attack in compound **1** at C₃, C₂₅, and C₃₂ are labeled in (Fig. 5). The computations show that the C₃ atom has the highest value between all the compounds which proves the highest practical result of this compound as an antioxidant in (Table 4).

Moreover, it has been observed that C₂, C₁₅ and C₂₂ are prone to radical attack in compound **16** because they show a higher positive value than other atoms. Also, compound **17** has been shown high tendency for radical attack, especially at atoms C₁ and C₅ which explains its antioxidant activity.

Structure activity relationship (SAR)

Generally, the starting material of tetrahydro benzo[*b*]thiophene-3-carbonitrile was exhibited greater antioxidant activity compared to the other prepared derivatives, as shown in (Fig. 6).

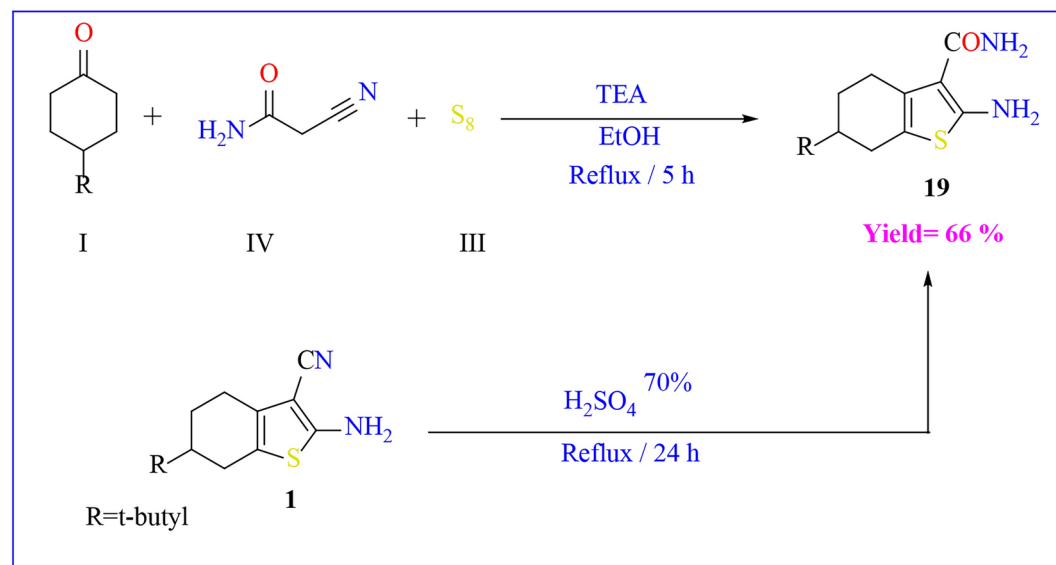
For pyrimidine derivatives

It was found that the reactivity of pyrimidine ring as antioxidants was increased when pyrimidine ring was substituted with electro donating group in position four as in compound **16** (R₁ = SH, R₂ = H) and in compound **17** (R₁ = NHHN₂, R₂ = H). By replacement of electro donating group to carbonyl group in the pyrimidine ring as in compound **20** (R₁ = CO, R₂ = Ph) and in compound **21** (R₁ = R₂ = CO) the oxidant activity was decreased. Also, the antioxidant activity was decreased by the replacement of carbonyl group into thiocarbonyl group as in compound **5** (R₁ = CS, R₂ = SH).

For N-substituted derivatives

It was found that the incorporation of amino group with alkyl as in compound **7** (R₃ = CH₃) was stronger in antioxidant activity than aryl group as in compound **6** (R₃ = Ph). Also, the substitution of amino group with R₃ = -N = (CN)CONH₂ as in compound **15** was increased the antioxidant activity than the substitution with R₃ = -N = (CN)CO₂C₂H₅ as in compound **13**.

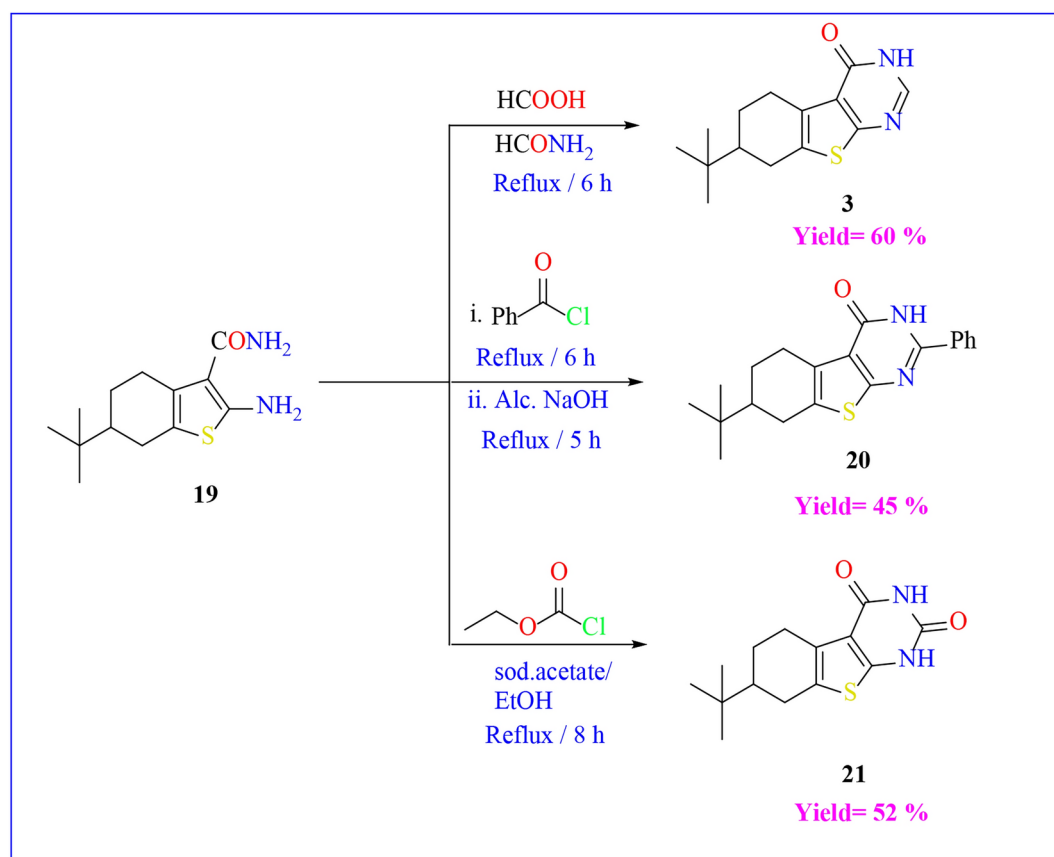
Furthermore, the condensation of amino group with aryl group containing electro donating group the antioxidant was increased as in compounds **9** (R₄ = *o*-bromo phenyl) and **11** (R₄ = 3-indolyl) than compound **10** (R₄ = *p*-nitro phenyl).



Scheme 7. Synthesis of compound **19**.

Compound	Docking score (Kcal/mol)	RMSD	Interaction	Binding site		Distance (Å)	E (kcal/mol)
				Ligand	Receptor		
1	-6.04	1.43	H-donor	S (14)	LEU557	4.12	-0.5
			H-donor	N (18)	ILE 559	3.16	-1.4
			pi-H	5-ring	GLY 605	4.92	-1
16	6.48-	1.51	H-acceptor	S (1)	VAL 418	3.63	-2.5
			H-acceptor	S (1)	VAL 465	3.69	-2.3
			H-acceptor	S (1)	VAL 465	3.93	-0.5
			pi-H	5-ring	ILE 559	4.79	-1.4
17	-6.94	2.18	H-donor	S (24)	VAL 604	3.34	-0.5
			H-donor	N (30)	VAL 512	3.04	-1.2
			pi-H	5-ring	ILE 559	4.9	-1.8
Ascorbic acid	5.21-	1.8	H-donor	O (1)	GLY 367	3.32	-1
			H-donor	O (12)	VAL 512	2.88	-2.3
			H-donor	O (17)	GLY 367	0.133	-1.4
			H-acceptor	O (12)	VAL 465	3.31	-0.8
			H-acceptor	O (14)	VAL 418	0.273	-0.8
			H-acceptor	O (14)	VAL 465	3.22	-0.5
PGE	5.398-	1.47	H-acceptor		VAL 465		-2.1
			H-acceptor		GLY 367		-2.5
			H-acceptor		VAL 606		-1.4
			H-acceptor		ILE 559		-0.5

Table 1. Docking binding free energies (ΔG) of the synthesized candidates with (Keap1) protein.



Scheme 8. Reactions of compound 19 with different electrophilic reagents.

Compound	1	16	17	Ascorbic acid
E_{HOMO} (eV)	-5.1200	-5.8667	-5.9358	-6.3715
E_{LUMO} (eV)	-0.9583	-1.8190	-1.1104	-1.0304
(ΔE) Energy gap (eV)	4.1616	4.0476	4.8253	5.3410
(I) Ionization energy (eV)	5.1200	5.8667	5.9358	6.3715
(A) Electron affinity (eV)	0.9583	1.8190	1.1104	1.0304
(η) Chemical hardness (eV)	2.0808	2.0238	2.4126	2.6705
(χ) Electronegativity (eV)	3.0392	3.8429	3.5231	3.7010
(S) Chemical softness (eV^{-1})	0.4805	0.4941	0.4144	0.3744
(μ) Electronic chemical potential (eV)	-3.0392	-3.8429	-3.5231	-3.7010
(ω) Electrophilicity index (eV)	2.2195	3.6485	2.5724	2.5645
(μ) Dipole moment (D)	4.4164	1.6939	3.8743	8.2249

Table 3. Quantum chemical parameters of the selected compounds with density functional theory (DFT) at B3LYP/6-31G (d,p) basis set.

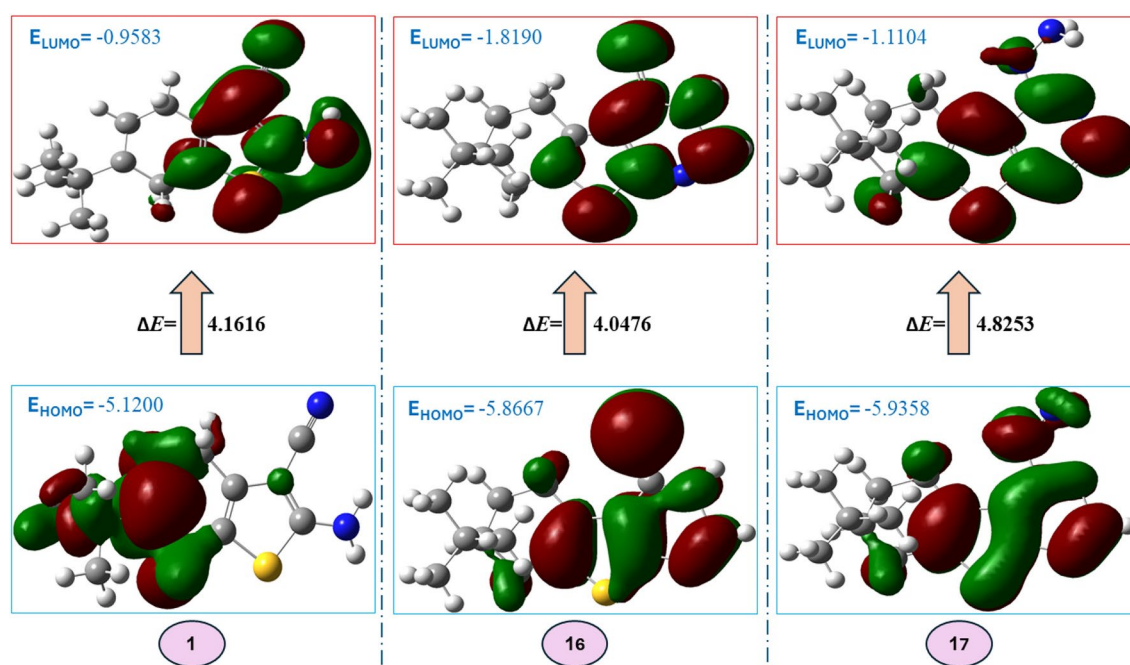


Fig. 4. Representation of HOMO and LUMO coefficient distribution and the energy gap in eV of compounds 1, 16, 17.

Experimental Materials

P-*t*-butyl cyclohexanone (98%) and malononitrile (99%) were supplied from Acros Organics and Alfa Aesar, respectively. Other chemicals and solvents used in syntheses and analytical assays were of analytical grade and were purchased from Sigma-Aldrich. Solvent drying was carried out according to standard techniques.

Instruments

Melting points were determined using a Griffin melting point apparatus. Fourier Transform Infrared (FT-IR) spectra were recorded from 400 to 4000 cm^{-1} using a Pye Unicam SP2000 infrared spectrophotometer with the KBr disc technique. Electron ionization mass spectra (EI-MS) were obtained using an AE1MS 902 mass spectrometer. Proton nuclear magnetic resonance (^1H NMR) spectra were recorded on a Varian Gemini instrument at 400 MHz, and the chemical shifts (δ) were reported in parts per million (ppm) relative to tetramethyl silane (TMS) as an internal standard in deuterated dimethyl sulfoxide (DMSO- d_6). Total Antioxidant Capacity Assay is a method used to measure the overall antioxidant capacity of the synthesized compounds. Antioxidants play a crucial role in protecting cells from damage caused by oxidative stress. Elemental analysis (C, H, N, and S) was performed at the Microanalytical Data Center at the Faculty of Science, Cairo University, Egypt. The progress of all reactions was monitored by TLC (thin layer chromatography, Merck) and spots were detected using a UV lamp (254 nm). Compounds 17 and 18 were synthesized previously as reported in the literature⁴⁶.

One-Sample Statistics

Compound	N	Mean (mg AAE/g compound) ¹	Std. deviation	Std. Error Mean
1	3	702.6400	2.91033	1.68028
2	3	381.7900	1.68573	.97326
3	3	151.6133	1.27017	.73333
4	3	121.1433	1.10500	.63797
5	3	105.3600	1.68573	.97326
6	3	111.9633	1.68028	.97011
7	3	455.9467	2.20500	1.27306
9	3	462.1833	.63509	.36667
10	3	244.1233	1.27017	.73333
11	3	310.5700	2.20000	1.27017
13	3	88.4700	1.68573	.97326
15	3	418.5000	1.10000	.63509
16	3	640.2333	1.68465	.97263
17	3	501.4700	2.29144	1.32296
18	3	313.8667	2.20505	1.27308
19	3	429.1467	2.77291	1.60094
20	3	258.6766	3.05505	1.76383
21	3	466.0000	2.00000	1.15470

V: strong

Strong

Moderate

Weak

V: weak

¹AAE (Ascorbic acid equivalent).**Table 4.** Total antioxidant capacity (TAC) of the synthesized compounds.

Compound	Atoms	f_k^0
1	C ₃	0.4599035
	C ₈	0.085998
	C ₁₇	0.0033245
	C ₂₅	0.1025715
	C ₃₂	0.1672675
	C ₃₃	0.00386
16	C ₂	0.1414435
	C ₃	0.050735
	C ₆	0.089216
	C ₁₅	0.123285
	C ₂₂	0.1508965
	C ₂₄	0.0603975
17	C ₁	0.1719425
	C ₅	0.387511
	C ₆	0.0477135
	C ₁₅	0.0453615
	C ₂₂	0.081895
	C ₂₃	0.039035

Table 5. Fukui Function value for a radical attack location.**Synthetic procedures***Synthesis of 2-(4-(tert-butyl)cyclohexylidene)malononitrile (1')*

To a solution of *p*-*t*-butyl cyclohexanone in absolute ethanol, (0.01 mol, 0.66 mL) of malononitrile was added, and the mixture was heated under reflux for 3 h. The reaction mixture was poured into ice. The formed precipitate

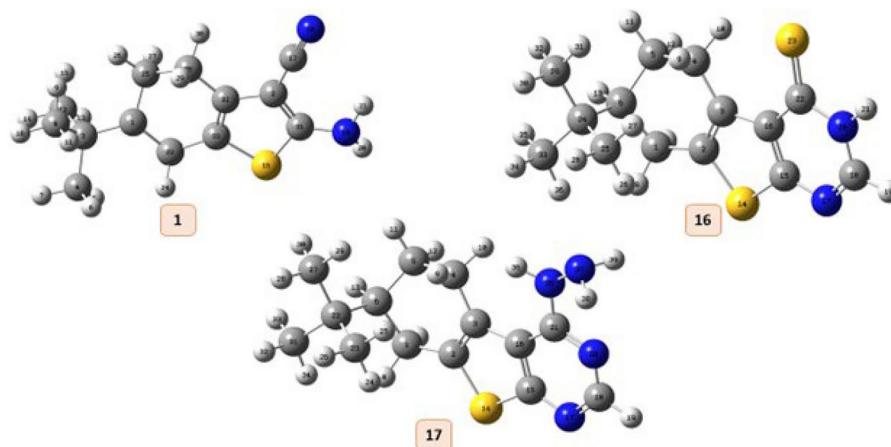


Fig. 5. Optimized geometric structure with atoms numbering of compounds 1, 16, and 17.

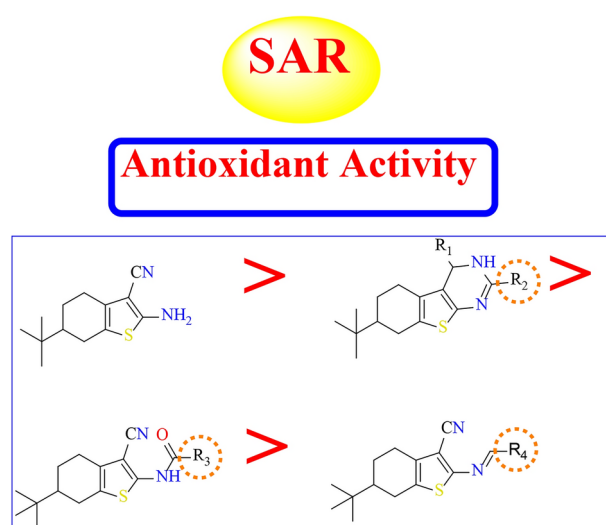


Fig. 6. Antioxidant activity of tetrahydro benzo[*b*]thiophene derivatives related to their chemical structures.

was filtered off, dried, and recrystallized from ethanol to give **1**. Yield (75%); mp $80\text{--}82\text{ }^{\circ}\text{C}$ (ethanol); FT-IR (KBr) ($\nu\text{ cm}^{-1}$): 1592 (C=C), 2954 (CH olefinic), 2228 (CN); 202 (M^+ , 10.12%). Anal. Calcd. For $\text{C}_{13}\text{H}_{18}\text{N}_2$ (202): C, 77.18; H, 8.97; N, 13.85. Found: C, 77.20; H, 9.00; N, 13.83.

2-amino-6-(*tert*-butyl)-4,5,6,7-tetrahydrobenzo[*b*]thiophene-3-carbonitrile (**1**)

A mixture of *t*-butyl cyclohexanone (0.01 mol, 1.54 g), malononitrile (0.01 mol, 0.66 g), and Sulphur element (0.01 mol, 0.32 g) in absolute ethanol (20 mL) containing (0.5 mL) of triethyl amine was heated under reflux condition for 2 h. the reaction mixture was poured into crushed ice / HCl with stirring. The formed precipitate was filtered off, dried, and recrystallized from ethanol to give **1**.

Yield (85%); mp $170\text{--}172\text{ }^{\circ}\text{C}$ (ethanol); FT-IR (KBr) ($\nu\text{ cm}^{-1}$): 1625 (C=C), 2959 (CH olefinic), 2201 (CN), 3323–3428 (NH_2); $^1\text{H-NMR}$ ($\text{DMSO-}d_6$) δ_{H} (ppm): 0.89 (s, 9H, *t*-butyl), 1.15–2.47 (m, 7H, H-cyclohexane), 6.93 (br.s., 2H, NH_2 , D_2O exchangeable); 234 (M^+ , 12.45%). Anal. Calcd. For $\text{C}_{13}\text{H}_{18}\text{N}_2\text{S}$ (234): C, 66.62; H, 7.74; N, 11.95. Found: C, 66.65; H, 7.71; N, 11.93.

7-(*tert*-butyl)-6,7,8,9-tetrahydrobenzo[4,5]thieno[3,2-*d*]pyrimidin-4-amine (**2**)

Treatment of compound **1** (0.01 mol, 2.34 g) with formamide (20 mL) was heated under reflux for 8 h. The reaction mixture was poured into crushed ice. The formed precipitate was filtered off, dried and recrystallized from benzene to obtain **2**.

Yield (65%); mp $228\text{--}230\text{ }^{\circ}\text{C}$ (benzene); FT-IR (KBr) ($\nu\text{ cm}^{-1}$): 1644 (C=N), 2958 (CH olefinic), 3313–3424 (NH_2); $^1\text{H-NMR}$ ($\text{DMSO-}d_6$) δ_{H} (ppm): 0.93 (s, 9H, *t*-butyl), 1.28–3.10 (m, 7H, H-cyclohexane), 4.61 (br.s., 2H, NH_2 , D_2O exchangeable), 8.32 (s, 1H, H-pyrimidine); MS, m/z (%): 261 (M^+ , 14.33%). Anal. Calcd. For $\text{C}_{14}\text{H}_{19}\text{N}_3\text{S}$ (261): C, 64.33; H, 7.33; N, 16.08. Found: C, 64.30; H, 7.35; N, 16.05.

7-(tert-butyl)-6,7,8,9-tetrahydrobenzo[4,5]thieno[3,2-d]pyrimidin-4(3H)-one (3)

To a solution of compound **1** (0.01 mol, 2.34 g) in formic acid (20 mL) was heated under reflux for 8 h. The reaction mixture was poured into crushed ice and neutralized with sodium carbonate solution. The formed precipitate was filtered off, dried and recrystallized from benzene to obtain **3**.

Yield (80%); mp = 252–254 °C (benzene); FT-IR (KBr) (ν cm⁻¹): 1593(C=N), 1658(C=O), 2947 (CH olefinic), 3157(NH); ¹H-NMR (DMSO-d₆) δ_{H} (ppm): 0.92 (s, 9H, t-butyl), 1.24–3.20(m, 7H, H-cyclohexane), 7.98 (s, 1H, H-pyrimidinone) 12.29 (br.s, H, NH, D₂O exchangeable); MS, m/z(%): 262(M⁺, 16.41%). Anal. Calcd. For C₂₂H₁₃Cl₂N₃ (262): C, 64.09; H, 6.92; N, 10.68. Found: C, 64.06; H, 6.90; N, 10.70.

1-(6-(tert-butyl)-3-cyano-4,5,6,7-tetrahydrobenzo[b]thiophen-2-yl)-3-phenylthiourea (4)

Treatment of compound **1** (0.01 mol, 2.34 g) with phenyl isothiocyanate (0.01 mol, 1.35 mL) in dioxane (20 mL) containing sodium metal (0.25 g) was heated under reflux 8 h. The reaction mixture was poured into crushed ice and neutralized with hydrochloric acid. The formed precipitate was filtered off, dried, and recrystallized from benzene/ethanol to afford **4**.

Yield (64%), mp = 210–212 °C, (benzene/ethanol); FT-IR (KBr) (ν cm⁻¹): 1613(C=C), 1242(C=S), 2205(CN), 2956 (CH olefinic), 3208(NH), 3288(NH); ¹H-NMR (DMSO-d₆) δ_{H} (ppm): 0.93 (s, 9H, t-butyl), 1.23–2.95 (m, 7H, H-cyclohexane), 7.24–7.77(m, 5H, H-Ar), 8.12 (br.s, H, NH, D₂O exchangeable), 8.19 (br.s, H, NH, D₂O exchangeable); MS, m/z: 369(M⁺, 79.91%). Anal. Calcd. For C₂₀H₂₃N₃S₂ (369): C, 65.00; H, 6.27; N, 11.37. Found: C, 65.03; H, 6.25; N, 11.40.

7-(tert-butyl)-5,6,7,8-tetrahydrobenzo[4,5]thieno[2,3-d]pyrimidine-2,4(1H,3H)-dithione (5)

The reaction of compound **1** (0.01 mol, 2.34 g) with carbon disulfide (5 mL) in dry pyridine (20 mL) was heated under reflux on a water bath for 24 h. Upon cooling, the precipitated solid was collected, dried, and recrystallized from benzene to afford **5**.

Yield (65%), mp = 290–292 °C, (benzene); FT-IR (KBr) (ν cm⁻¹): 1600(C=C), 1235 (C=S), 3108(NH), 3379(NH); ¹H-NMR (DMSO-d₆) δ_{H} (ppm): 0.92 (s, 9H, t-butyl), 1.24–3.20 (m, 7H, H-cyclohexane), 12.29 (br.s, H, NH, D₂O exchangeable), 13.23 (br.s, H, NH, D₂O exchangeable); MS, m/z: 310(M⁺, 33.58%). Anal. Calcd. For C₁₄H₁₈N₂S₃ (341): C, 54.16; H, 5.84; N, 9.02. Found: C, 54.13; H, 5.81; N, 9.05.

N-(6-(tert-butyl)-3-cyano-4,5,6,7-tetrahydrobenzo[b]thiophen-2-yl)benzamide (6)

A mixture of compound **1** (0.01 mol, 2.34 g) and benzoyl chloride (20 mL) was heated under reflux for 7 h. After evaporation of the solvent, wash the formed precipitate with petroleum ether (80C-100C) and recrystallized from benzene to give **6**.

Yield (72%), mp = 180–182 °C, (benzene); FT-IR (KBr) (ν cm⁻¹): 1667 (C=O), 2216 (CN), 3245 (NH); ¹H-NMR (DMSO-d₆) δ_{H} (ppm): ¹H-NMR (DMSO-d₆) δ_{H} (ppm): 0.93 (s, 9H, t-butyl), 1.27–2.75 (m, 7H, H-cyclohexane), 7.55–7.96 (m, 5H, H-Ar), 11.70 (br.s, H, NH, D₂O exchangeable); MS, m/z: 338(M⁺, 11.23%). Anal. Calcd. For C₂₀H₂₂N₂OS (338): C, 70.97; H, 6.55; N, 8.28. Found: C, 80.00; H, 6.52; N, 8.25.

6-(tert-butyl)-2-(1,3-dioxoisindolin-2-yl)-4,5,6,7-tetrahydrobenzo[b]thiophene-3-carbonitrile (7)

A mixture of compound **1** (0.01 mol, 2.34 g) and phthalic anhydride (0.01 mol, 1.48 g) in glacial acetic acid (20 mL) was refluxed for 8 h. The reaction mixture was poured into crushed ice. The formed precipitate was filtered off, dried, and recrystallized from toluene to afford **7**.

Yield (60%); mp = 242–244 °C (toluene); FT-IR (KBr) (ν cm⁻¹): 1697 (C=O), 2217 (CN), 2948 (CH olefinic), 3225 (NH); ¹H-NMR (DMSO-d₆) δ_{H} (ppm): 0.90 (s, 9H, t-butyl), 1.22–2.66 (m, 7H, H-cyclohexane), 2.16 (s, 3H, CH₃), 11.49 (br.s, H, NH, D₂O exchangeable); MS, m/z: 276 (M⁺, 21.22%). Anal. Calcd. For C₁₅H₂₀N₂OS (276): C, 65.18; H, 7.29; N, 10.14. Found: C, 65.15; H, 7.31; N, 10.11.

2-amino-7-(tert-butyl)-4-imino-3,4,5,6,7,8-hexahydrobenzo[4,5]thieno[2,3-b]pyridine-3-carbonitrile (8)

To a solution of compound **1** (0.01 mol, 2.34 g) in absolute ethanol (25 mL) containing drops of piperidine (3 drops), malononitrile (0.1 mol, 0.66 g) was added and then the reaction mixture was allowed to reflux for 7 h. the reaction mixture was poured into crushed ice/ HCl. The formed precipitate was filtered off, dried and recrystallized from ethanol to obtain **8**.

Yield (70%); mp = 230–232 °C (ethanol); FT-IR (KBr) (ν cm⁻¹): 1625 (C=N), 2215 (CN), 3221 (NH), 3268–3321 (NH₂); ¹H-NMR (DMSO-d₆) δ_{H} (ppm): 0.88–0.90 (s, 9H, t-butyl), 1.04–2.67 (m, 7H, H-cyclohexane), 2.17 (s, 1H, CH pyridine), 6.92 (br.s, 2H, NH₂, D₂O exchangeable), 11.50 (br.s, H, NH, D₂O exchangeable); MS, m/z: 300(M⁺, 13.65%). Anal. Calcd. For C₁₆H₂₀N₄S (300): C, 63.97; H, 6.71; N, 18.65. Found: C, 64.00; H, 6.69; N, 18.67.

General method for compounds 9, 10 and 11

To a hot solution of compound **1** (0.01 mol, 2.34 g) in ethanol (20 mL) containing a few drops of piperidine (5 drops), *o*-bromo benzaldehyde, and /or *p*-nitro benzaldehyde and/ or indole-3-carboxaldehyde (0.01 mol) was added, and the reaction mixture was heated under reflux for 4 h. The reaction mixture was poured into crushed ice and neutralized with hydrochloric acid. The formed precipitate was filtered off, dried, and recrystallized from proper organic solvent to afford the corresponding Schiff's base **9**, **10**, and **11**.

3-((2-bromobenzylidene)amino)-6-(tert-butyl)-4,5,6,7-tetrahydrobenzo[b]thiophene-2-carbonitrile (9)

Yield (65%); mp = 162–164 °C (toluene); FT-IR (KBr) (ν cm⁻¹): 1582(C=C), 1629(C=N), 2219(CN); ¹H-NMR (DMSO-d₆) δ_{H} (ppm): 0.93 (s, 9H, t-butyl), 1.27–2.83(m, 7H, H-cyclohexane), 7.50–8.16 (m, 4H, H-Ar), 8.76(s,

1H, olefinic N=C(H)); MS, m/z: 401(M⁺, 2.92%). Anal. Calcd. For C₂₀H₂₁BrN₂S (401): C, 59.85; H, 5.27; N, 6.98. Found: C, 59.82; H, 5.30; N, 6.95.

6-(*tert*-butyl)-3-(4-nitrostyryl)-4,5,6,7-tetrahydrobenzo[*b*]thiophene-2-carbonitrile (10)

Yield (70%); mp = 216–218 °C (ethanol); FT-IR (KBr) (ν cm⁻¹): 1557(C=C), 1598(C=N), 2218(CN); ¹H-NMR (DMSO-d₆) δ_H (ppm): 0.88–0.93 (s, 9H, *t*-butyl), 1.29–2.84(m, 7H, H-cyclohexane), 8.19–8.21 (d, 2H, H-Ar), 8.36–8.38 (d, 2H, H-Ar), 8.77(s, 1H, olefinic N=C(H)); MS, m/z: 367(M⁺, 34.65%). Anal. Calcd. For C₂₀H₂₁N₃O₂S (367): C, 65.37; H, 5.76; N, 11.44. Found: C, 65.40; H, 5.73; N, 11.46.

3-(((1*H*-indol-3-yl)methylene)amino)-6-(*tert*-butyl)-4,5,6,7-tetrahydrobenzo[*b*]thiophene-2-carbonitrile (11)

Yield (60%); mp = 210–212 °C (toluene); FT-IR (KBr) (ν cm⁻¹): 1564(C=C), 1596(C=N), 2212(CN), 3328(NH); ¹H-NMR (DMSO-d₆) δ_H (ppm): 0.88–0.93 (s, 9H, *t*-butyl), 1.29–2.75(m, 7H, H-cyclohexane), 7.23–8.40 (m, 5H, H-Ar), 8.71(s, 1H, olefinic N=C(H)), 12.09 (br.s., H, NH D₂O exchangeable); MS, m/z: 361(M⁺, 25.53%). Anal. Calcd. For C₂₂H₂₃N₃S (361): C, 73.09; H, 6.41; N, 11.62. Found: C, 73.11; H, 6.44; N, 11.65.

General method for compounds 13 and 14

The corresponding diazonium chloride **12** was prepared in situ from 2-aminothiophene-3-carbonitrile derivative **1** (0.01 mol, 2.34 g) in conc. HCl (10 mL) and cold solution of sodium nitrite (0.01 mol, 0.69 g in 15 mL of H₂O) with continuous stirring. To cold mixture of ethyl cyanoacetate (0.01 mol, 1.13 mL) and/or ethyl acetoacetate (0.01 mol, 1.30 mL) in 20 mL ethanol and sodium acetate (0.02 mol, 1.6 g), a cold aqueous solution of diazonium salt **12** was added dropwise with stirring at 0–5°C for 2 h. The solid product obtained was filtered off, dried, and recrystallized from benzene to afford compounds **13** and **14** respectively.

Ethyl-2-(2-(6-(*tert*-butyl)-3-cyano-4,5,6,7-tetrahydrobenzo[*b*]thiophen-2-yl)hydrazono)-2-cyanoacetate (13)

Yield (55%); mp = 174–176 °C (benzene); FT-IR (KBr) (ν cm⁻¹): 1622(C=N), 1732(C=O), 2224(CN), 3424(NH); MS, m/z: 358(M⁺, 12.41%). Anal. Calcd. For C₁₈H₂₂N₄O₂S (358) : C, 60.31; H, 6.19; N, 15.63. Found: C, 60.35; H, 6.21; N, 15.65.

Ethyl-2-(2-(6-(*tert*-butyl)-3-cyano-4,5,6,7-tetrahydrobenzo[*b*]thiophen-2-yl)hydrazono)-3-oxobutanoate (14)

Yield (50%); mp = 108–110 °C (benzene); FT-IR (KBr) (ν cm⁻¹): 1632(C=N), 1696(C=O), 1740(C=O), 2225(CN), 3363(NH); MS, m/z: 375(M⁺, 25.38%). Anal. Calcd. For C₁₉H₂₅N₃O₃S (375): C, 60.78; H, 6.71; N, 11.19. Found: C, 60.80; H, 6.73; N, 11.21.

N-(6-(*tert*-butyl)-3-cyano-4,5,6,7-tetrahydrobenzo[*b*]thiophen-2-yl)-2-hydrazinyl-2-oxoacetohydrazonoyl cyanide (15)

A mixture of compound **13** (0.01 mol, 3.58 g), and hydrazine hydrate (0.02 mol, 1 mL) in absolute ethanol (20 mL) was heated under reflux for 6 h. The reaction mixture was cooled, and the formed precipitate was filtered off, dried, and recrystallized from ethanol to afford **15**.

Yield (60%); mp = 156–158 °C (ethanol); FT-IR (KBr) (ν cm⁻¹): 1586 (C=N), 1623 (C=O), 2199 (CN), 3198–3314 (2NH, NH₂); ¹H-NMR (DMSO-d₆) δ_H (ppm): 0.89 (s, 9H, *t*-butyl), 1.15–2.47 (m, 7H, H-cyclohexane), 5.42 (br.s., 2H, NH₂, D₂O exchangeable), 7.64 (br.s., 1H, NH, D₂O exchangeable), 12.41 (br.s., 1H, NH, D₂O exchangeable); MS, m/z: 344(M⁺, 42.12%). Anal. Calcd. For C₁₆H₂₀N₆OS (344): C, 55.79; H, 5.85; N, 24.40. Found: C, 55.76; H, 5.81; N, 24.43.

7-(*tert*-butyl)-6,7,8,9-tetrahydrobenzo[4,5]thieno[3,2-*d*]pyrimidine-4(3*H*)-thione (16)

The reaction of compound **3** (0.01 mol, 2.62 g) with phosphorus pentasulfide (0.01 mol, 4.44 g) in dry toluene was heated under reflux at 5 h and left to cool. The formed precipitate was collected and recrystallized from ethanol to afford compound **16**.

Yield (65%); mp = 236–238 °C (ethanol); FT-IR (KBr) (ν cm⁻¹): 1206(C=S), 1617(C=N), 3125(NH); MS, m/z: 278(M⁺, 21.73%). Anal. Calcd. For C₁₄H₁₈N₂S₂ (278): C, 60.39; H, 6.52; N, 10.06. Found: C, 60.41; H, 6.55; N, 10.09.

7-(*tert*-butyl)-4-hydrazinyl-6,7,8,9-tetrahydrobenzo[4,5]thieno[3,2-*d*]pyrimidine (17)

To a solution of compound **16** (0.1 mol, 2.78 g) in 20 mL absolute ethanol, hydrazine hydrate (2 mL) was added and refluxed for 6 h. After cooling, the reaction mixture was poured into ice/ hydrochloric acid then the formed solid was filtered off, dried, and recrystallized from toluene to give compound **17**.

Yield (60%); mp = 180–182 °C (ethanol); FT-IR (KBr) (ν cm⁻¹): 1571(C=C), 1629 (C=N), 3196(NH), 3313–3392 (NH₂); ¹H-NMR (DMSO-d₆) δ_H (ppm): 0.93 (s, 9H, *t*-butyl), 1.28–3.10(m, 7H, H-cyclohexane), 4.61 (br.s., 2H, NH₂, D₂O exchangeable), 7.88 (br.s., 1H, NH, D₂O exchangeable), 8.32(s, 1H, H-pyrimidine); MS, m/z: 276(M⁺, 9.20%). Anal. Calcd. For C₁₄H₂₀N₄S (276): C, 60.84; H, 7.29; N, 20.27. Found: C, 60.81; H, 7.31; N, 20.25.

Ethyl 2-((7-(*tert*-butyl)-6,7,8,9-tetrahydrobenzo[4,5]thieno[3,2-*d*]pyrimidin-4-yl)thio)acetate (18)

A mixture of compound **16** (0.01 mol, 2.78 g) and ethyl chloroacetate (0.01 mol, 1.22 mL) in the presence of dry acetone containing anhydrous potassium carbonate (0.01 mol, 1.38 g) was heated under reflux on a water bath for 24 h. Evaporation of the solvent and washing of the formed precipitate with petroleum ether and then filtered off, dried, and recrystallized from ethanol to obtain compound **18**.

Yield (54%); mp = 98–100 °C (ethanol); FT-IR (KBr) (ν cm⁻¹): 1561(C=C), 1595(C=N), 1746(C=O), 2944 (CH olefinic); ¹H-NMR (DMSO-d₆) δ_H (ppm): 0.93 (s, 9H, *t*-butyl), 1.17–1.21(t, 3H, CH₃), 1.32–3.28(m, 7H,

H-cyclohexane), 4.10–4.16(q, 2H, CH₃), 8.65(s, 1H, H-pyrimidine); MS, m/z: 364(M⁺, 26.88%). Anal. Calcd. For C₁₈H₂₄N₂O₂S₂ (364): C, 59.31; H, 6.64; N, 7.69. Found: C, 59.34; H, 6.61; N, 7.72.

2-amino-6-(tert-butyl)-4,5,6,7-tetrahydrobenzo[b]thiophene-3-carboxamide (19)

A mixture of t-butyl cyclohexanone (0.01 mol, 1.54 g), cyano acetamide (0.01 mol, 0.84 g) and Sulphur element (0.01 mol, 0.32 g) in absolute ethanol (20 mL) containing (0.5 mL) of triethyl amine was heated under reflux condition for 5 h. the reaction mixture was poured into crushed ice / HCl with stirring. The formed precipitate was filtered off, dried and recrystallized from ethanol to give **19**.

Yield (66%); mp. = 218–220 °C (ethanol); FT-IR (KBr) (ν cm⁻¹): 1650 (C=O), 3322–3497(2 NH₂); ¹H-NMR (DMSO-d₆) δ H (ppm): 0.89 (s, 9H, t-butyl), 1.15–2.47(m, 7H, H-cyclohexane), 7.19(br.s., 2H, NH₂, D₂O exchangeable), 7.88(br.s., 2H, NH₂, D₂O exchangeable); MS, m/z: 252(M⁺, 20.48%). Anal. Calcd. For C₁₃H₂₀N₂OS (252): C, 61.87; H, 7.99; N, 11.10. Found: C, 61.84; H, 8.02; N, 10.13.

Another method for synthesis of 19

To a solution of compound **1** (0.01 mol, 2.34 g) in sulphuric acid 70% (15 mL) was heated in water bath for 24 h. The reaction mixture was poured into crushed ice with continuous stirring. The formed precipitate was filtered off, dried, and recrystallized from ethanol to give **19**.

7-(tert-butyl)-6,7,8,9-tetrahydrobenzo[4,5]thieno[3,2-d]pyrimidin-4(3H)-one (3)

Compound **19** (0.01 mol, 2.52 g) was added to a mixture of Formic acid/ Formamide (10:5 mL). the reaction mixture was allowed to reflux for 6 h and cooled. The precipitate that formed was filtered off, dried, and recrystallized from benzene to give **3**. Yield (60%).

7-(tert-butyl)-2-phenyl-5,6,7,8-tetrahydrobenzo[4,5]thieno[2,3-d]pyrimidin-4(3H)-one (20)

Fusion of compound **19** (0.01 mol, 2.52 g) with benzoyl chloride (10 mL) was heated under reflux on the hot plate for 6 h. The reaction mixture was left to evaporate the solvent, and then (15 mL) of aqueous alcoholic sodium hydroxide (25%) was added and complete refluxing for 5 h. The formed precipitate was washed with petroleum ether 60–80 to afford compound **20**.

Yield (45%); mp. = 114–116 °C (toluene); FT-IR (KBr) (ν cm⁻¹): 1580(C=C), 1601(C=N), 1679(C=O), 3059 (CH aromatic) 3169 (NH); ¹H-NMR (DMSO-d₆) δ H (ppm): 0.87,0.91 (s, 9H, t-butyl), 1.21–2.28(m, 7H, H-cyclohexane), 7.47–7.96(m, 5H, Ar-H), 12.99 (br.s., 1H, NH, D₂O exchangeable); MS, m/z: 338(M⁺, 21.35%). Anal. Calcd. For C₂₀H₂₂N₂OS (338): C, 70.97; H, 6.55; N, 8.28. Found: C, 71.00; H, 6.58; N, 8.25.

7-(tert-butyl)-5,6,7,8-tetrahydrobenzo[4,5]thieno[2,3-d]pyrimidine-2,4(1H,3H)-dione (21)

A mixture of compound **19** (0.01 mol, 2.52 g) and ethyl chloro formate (0.01 mol, 1.08 mL) in absolute ethanol (20 mL) containing fused sodium acetate (0.01 mol, 0.82 g) was heated for 8 h. The reaction mixture was poured into crushed ice/ HCl. The formed precipitate was filtered off, dried, and recrystallized from ethanol to afford **21**.

Yield (52%); mp. = 128–130 °C (ethanol); FT-IR (KBr) (ν cm⁻¹): 1657(2 C=O), 3207(2 NH); ¹H-NMR (DMSO-d₆) δ H (ppm): 0.84, 0.92 (s, 9H, t-butyl), 1.14–2.32 (m, 7H, H-cyclohexane), 11.32 (br.s., 1H, NH, D₂O exchangeable), 12.42 (br.s., 1H, NH, D₂O exchangeable); MS, m/z: 278(M⁺, 35.86%). Anal. Calcd. For C₁₄H₁₈N₂O₂S (278): C, 60.41; H, 6.52; N, 10.06. Found: C, 60.44; H, 6.49; N, 10.09.

Determination of total antioxidant capacity (TAC)

The antioxidant activity of each compound was determined according to the phosphomolybdenum method using ascorbic acid as standard. This assay is based on the reduction of Mo (VI) to Mo (V) by the sample analyte and the subsequent formation of a green-colored [phosphate=Mo (V)] complex at acidic pH with maximal absorption at 695 nm. In this method, 0.5 ml of each compound (200 μ g/ml) in methanol was combined in dried vials with 5 ml of reagent solution (0.6 M sulfuric acid, 28 mM sodium phosphate, and 4 mM ammonium molybdate). The vials containing the reaction mixture were capped and incubated in a thermal block at 95 °C for 90 min. After the samples had cooled at room temperature, the absorbance was measured at 695 nm against a blank. The blank consisted of all reagents and solvents without the sample, and it was incubated under the same conditions. All experiments were carried out in triplicate. The antioxidant activity of the sample was expressed as the number of ascorbic acid equivalents (AAE)^{66–70}.

Molecular docking

To clarify the mode of action and predict the potency of the tested drugs, molecular docking studies were performed, emphasizing the interactions between ligands and receptors. Chemdraw 20.0 (CambridgeSoft) from Perkin Inc. was used for drawing ligands and tested compounds. To enhance the fitting and docking results, the Wave Function Spartan v 14.0 program⁷¹ was utilized to optimize the geometries and minimize the global energies of both the ligands and the tested compounds.

In the docking study, the crystal structure of the binding protein. The X-ray crystal structure of the Keap1 (Kelch-like ECH-associated protein 1) protein was retrieved from the Protein Data Bank (PDB: 7C5E). Auto Dock Vina was employed to perform the molecular docking study, focusing on the interaction between ascorbic acid, and the tested compounds **1**, **16**, **17** with Keap1 (Kelch-like ECH-associated protein 1). To prepare the protein receptor, necessary steps such as 3D hydrogenation and energy minimization were carried out^{72,73}. The visualization process was conducted using the PyMOL program⁷⁴.

DFT calculations

The Gaussian 09W program⁷⁵ was employed for Density Functional Theory (DFT) calculations. The calculations were performed at the B3LYP level, a hybrid exchange functional that combines Becke's three-parameter method (local, non-local, and Hartree–Fock) with the Lee–Yang–Parr correlation functional^{76,77}.

For the full geometry optimization of the studied compounds, the 6–31 + G(d,p) basis set was employed. This basis set includes 'd' polarization functions for heavy atoms and 'p' polarization functions for hydrogen atoms. Additionally, diffuse functions were incorporated for both hydrogen and heavy atoms to improve accuracy in describing the optimized structures and ground state properties.

To assess the chemical reactivity of compounds **1**, **16**, **17** and reference drugs, several theoretical descriptors based on conceptual Density Functional Theory (DFT) were determined. These descriptors include the Lowest Unoccupied (vacant) Molecular Orbital (LUMO) energy (ELUMO), the Highest Occupied Molecular Orbital (HOMO) energy (EHOMO), the electronegativity (χ), the global softness (S), and the hardness (η). It is important to note that these descriptors were calculated based on the optimized molecular structures. It should be emphasized that the descriptors associated with the frontier molecular orbitals (FMO) were determined using a simplified approach within the framework of the Koopmans approximation⁷⁸.

Conclusions

Various heterocyclic frameworks, including pyrimidine-thione, pyrimidinone, and pyridine derivatives, were effectively synthesized from the 2-amino thiophene-3-carbonitrile derivative **1** through reactions with diverse nitrogen and carbon nucleophiles. The chemical structures of all the synthesized compounds were verified through elemental and spectral analyses. The ultimate heterocyclic product was notably influenced by the reaction conditions, such as the reaction medium. The investigation of the total antioxidant capacity (TAC) revealed that compound **1** displays a robust antioxidant effect, comparable to that of ascorbic acid. Moreover, compounds **16** and **17** show substantial activity, exceeding the potency of the first compound. In conclusion, the gathered data indicate the capability of compound **1** to produce novel heterocyclic frameworks with strong antioxidant properties, suggesting potential applications in the treatment of diseases associated with oxidative stress. Furthermore, future research should include *in vivo* antioxidant experiments and additional *in vitro* antioxidant assays, such as NO and O₂^{•-}, to validate the antioxidant potential of these novel heterocyclic frameworks. *In silico* studies, involving molecular docking and DFT calculations were conducted for the most antioxidant-active compounds, namely **1**, **16**, and **17**, and were compared with ascorbic acid as a reference antioxidant.

Data availability

The data that supports the findings of this study are available in the supplementary material of this article.

Received: 7 July 2024; Accepted: 24 September 2024

Published online: 09 November 2024

References

- Briel, D., Rybak, A., Kronbach, C. & Unverferth, K. Substituted 2-aminothiopen-derivatives: A potential new class of GluR6-Antagonists. *Eur. J. Med. Chem.* **45**(1), 69–77 (2010).
- Maradiya, H. R. Synthesis of azobenzene [b] thiophene derivatives and their dyeing performance on polyester fibre. *Turk. J. Chem.* **25**(4), 441–450 (2001).
- Sabnis, R., Rangnekar, D. & Sonawane, N. 2-Aminothiophenes by the Gewald reaction. *J. Heterocycl. Chem.* **36**(2), 333–345 (1999).
- Koike, K. et al. Echinothiophene, a novel benzothiophene glycoside from the roots of *Echinops grijissii*. *Org. Lett.* **1**(2), 197–198 (1999).
- Luna, I. S. et al. Design, synthesis and antifungal activity of new Schiff bases bearing 2-aminothiophene derivatives obtained by molecular simplification. *J. Braz. Chem. Soc.* **32**, 1017–1029 (2021).
- Ibrahim, B. A. & Mohareb, R. M. Uses of ethyl benzoyl acetate for the synthesis of thiophene, pyran, and pyridine derivatives with antitumor activities. *J. Heterocycl. Chem.* **57**(11), 4023–4035 (2020).
- Nayak, S. G., Poojary, B. & Kamat, V. Archiv der Pharmazie Novel pyrazole-clubbed thiophene derivatives via Gewald synthesis as antibacterial and anti-inflammatory agents. *Arch. Pharm.* **353**(12), 2000103 (2020).
- Abed, N. A., Hammouda, M. M., Ismail, M. A. & Abdel-Latif, E. Synthesis of new heterocycles festooned with thiophene and evaluating their antioxidant activity. *J. Heterocycl. Chem.* **57**(12), 4153–4163 (2020).
- Khalifa, M. E. & Algothami, W. M. Gewald synthesis, antitumor profile and molecular modeling of novel 5-acetyl-4-((4-acetylphenyl) amino)-2-aminothiophene-3-carbonitrile scaffolds. *J. Mol. Struct.* **1207**, 127784 (2020).
- Bozorov, K., Nie, L. F., Zhao, J. & Aisa, H. A. 2-Aminothiophene scaffolds: Diverse biological and pharmacological attributes in medicinal chemistry. *Eur. J. Med. Chem.* **140**, 465–493 (2017).
- Lee, K. et al. Efficacious and orally bioavailable thrombin inhibitors based on a 2, 5-thienylamidine at the P1 position: discovery of N-carboxymethyl-d-diphenylalanyl-l-prolyl [(5-amidino-2-thienyl) methyl] amide. *J. Med. Chem.* **46**(17), 3612–3622 (2003).
- Sridhar, M., Rao, R. M., Baba, N. H. & Kumbhare, R. M. Microwave accelerated Gewald reaction: synthesis of 2-aminothiophenes. *Tetrahedron Lett.* **48**(18), 3171–3172 (2007).
- Zhou, H. C. & Wang, Y. Recent researches in triazole compounds as medicinal drugs. *Curr. Med. Chem.* **19**(2), 239–280 (2012).
- Sabnis, R. W., Rangnekar, D. W. & Sonawane, N. D. 2-Aminothiophenes by the Gewald reaction. *J. Heterocycl. Chem.* **36**, 333–345 (1999).
- Gewald, K., Schinke, E. & Bottcher, H. Heterocyclen aus CH-aciden Nitrilen. VIII. 2-Amino-thiophene aus methylenaktiven Nitrilen, carbonylverbindungen und schwefel. *Chem. Ber.* **99**, 94–100 (1966).
- Sabnis, R. W. The Gewald reaction in dye chemistry. *Color. Technol.* **132**(1), 49–82 (2016).
- Puterova, Z., Krutosikova, A. & Vegh, D. Gewald reaction: synthesis, properties and applications of substituted 2-aminothiophenes. *Arkivoc* **1**, 209–246 (2010).
- Aman, B. A., Preety, S. & Shamsheer, S. B. 2-Aminothiophenes: a review on synthetic routes and applications (biological/syntheses). *Am. J. Pharm. Tech. Res.* **7**(1), 57–78 (2017).

19. Li, P., Liu, Y., Wang, L., Tao, M. & Zhang, W. Modified polyacrylonitrile fiber as a renewable heterogeneous base catalyst for Henry reaction and Gewald reaction in water. *J. Appl. Polym. Sci.* **135**(11), 45992 (2018).
20. El-Borai, M. A., Rizk, H. F., Ibrahim, S. A. & Fares, A. K. An eco-friendly synthesis and biological screening of fused heterocyclic compounds containing a thiophene moiety via gewald reaction. *J. Heterocycl. Chem.* **56**(10), 2787–2795 (2019).
21. Cohen, S. M., Duffy, J. L. & Miller, C. Direct observation (NMR) of the efficacy of glucagon receptor antagonists in murine liver expressing the human glucagon receptor. *Bioorg. Med. Chem.* **14**, 1506–1517 (2006).
22. Yen, M. S. & Wang, I. J. Synthesis and absorption spectra of hetarylazo dyes derived from coupler 4-aryl-3-cyano-2-aminothiophenes. *Dyes Pigm.* **61**, 243–250 (2004).
23. Vriezema, D. M. et al. Vesicles and polymerized vesicles from thiophene-containing rod–coil block copolymers. *Angew. Chem. Int. Ed.* **42**(7), 772–776 (2003).
24. Dore, K. et al. Fluorescent polymeric transducer for the rapid, simple, and specific detection of nucleic acids at the zeptomole level. *J. Am. Chem. Soc.* **126**, 4240–4244 (2004).
25. Gewald, K. Zur reaktion von α -oxo-mercaptanen mit nitrilen. *Angew. Chem.* **73**, 114 (1961).
26. Lahsasni, S. et al. Synthesis, characterization, and antibacterial and anti-inflammatory activities of new pyrimidine and thiophene derivatives. *J. Chem.* **2018**(1), 8536063 (2018).
27. Gevorgyan, G. A., Hakobyan, N. Z., Hovakimyan, S. S., Melkonyan, A. G. & Panosyan, G. A. Synthesis and biological activity of β -Aminoketones, secondary aminopropanols and oximes of 2-aminothiophene series. *Russ. J. Chem.* **89**, 2328–2332 (2019).
28. El Bialy, S. A. A. & Gouda, M. A. Cyanoacetamide in heterocyclic chemistry: Synthesis, antitumor and antioxidant activities of some new benzothiophenes. *J. Heterocycl. Chem.* **48**, 1280 (2011).
29. Gouda, M. A. & Abu-Hashem, A. A. Synthesis, characterization, antioxidant and antitumor evaluation of some new thiazolidine and thiazolidinone derivatives. *Arch. Pharm.* **344**(3), 170–177 (2011).
30. Elmongy, E., Kedr, M., Abotaleb, N. & Abbas, S. Design and synthesis of new thienopyrimidine derivatives along with their antioxidant activity. *Egypt. J. Chem.* **64**(11), 6857–6867 (2021).
31. El-Bordany, E. A., Abdel Aziz, A., Abou-Elmagd, W. S. I. & Hashem, A. I. Synthesis and spectroscopic characterization of some novel pyrazoloquinoline, pyrazolyltetrazine, and thiazolidinone derivatives. *J. Heterocycl. Chem.* **55**(1), 291–296 (2018).
32. Ghareeb, E. A., Mahmoud, N. F. H., El-Bordany, E. A. & El-Helw, E. A. E. Synthesis, DFT, and eco-friendly insecticidal activity of some N-heterocycles derived from 4-((2-oxo-1, 2-dihydroquinolin-3-yl) methylene)-2-phenyloxazol-5 (4H)-one. *Bioorg. Chem.* **112**, 104945 (2021).
33. Mahmoud, N. F. H. & Ghareeb, E. A. Synthesis of novel substituted tetrahydropyrimidine derivatives and evaluation of their pharmacological and antimicrobial activities. *J. Heterocycl. Chem.* **56**(1), 81–91 (2019).
34. Mahmoud, N. F. H. & El-Saghier, A. M. Multi-component reactions, solvent-free synthesis of substituted pyrano-pyridopyrimidine under different conditions using ZnO nanoparticles. *J. Heterocycl. Chem.* **56**(6), 1820–1824 (2019).
35. Mahmoud, N. F. H., Elsayed, G. A. & Ismail, M. F. Synthesis of various fused heterocyclic rings from oxoindenyl esters and their pharmacological and antimicrobial evaluations. *J. Heterocycl. Chem.* **55**(2), 465–474 (2018).
36. Mahmoud, N. F. H. & El-Sewedy, A. Facile synthesis of novel heterocyclic compounds based on pyridine moiety with pharmaceutical activities. *J. Heterocycl. Chem.* **57**(4), 1559–1572 (2020).
37. Gouda, M. A. S., Salem, M. A. I. & Mahmoud, N. F. H. 3D-pharmacophore study molecular docking and synthesis of pyrido [2, 3-d] pyrimidine-4 (1 H) dione derivatives with in vitro potential anticancer and antioxidant activities. *J. Heterocycl. Chem.* **57**(11), 3988–4006 (2020).
38. Mahmoud, N. F. H. & Balamon, M. G. Synthesis of various fused heterocyclic rings from thiazolopyridine and their pharmacological and antimicrobial evaluations. *J. Heterocycl. Chem.* **57**(8), 3056–3070 (2020).
39. Mahmoud, N. F. H. & Elsayed, G. A. Molecular docking and biological assessment of substituted phthalazin-1 (2H)-one derivatives. *J. Heterocycl. Chem.* **57**(4), 1845–1862 (2020).
40. Hemdan, M. M. & El-Bordany, E. A. Use of dodecanoyl isothiocyanate as building block in synthesis of target benzothiazine, quinazoline, benzothiazole and thiourea derivatives. *Chem. Pap.* **70**(8), 1117–1125 (2016).
41. El-Hashash, M. A., El-Naggar, A. M., El-Bordany, E. A., Marzouk, M. I. & Nawar, T. M. S. 6-Iodo-2-isopropyl-4 H-3, 1-benzoxazin-4-one as building block in heterocyclic synthesis. *Synth. Commun.* **46**(24), 2009–2021 (2016).
42. El-Bordany, E. A. & Ali, R. S. Synthesis of new benzoxazinone, quinazolinone, and pyrazoloquinazolinone derivatives and evaluation of their cytotoxic activity against human breast cancer cells. *J. Heterocycl. Chem.* **55**(5), 1223–1231 (2018).
43. El-Hashash, M. A. et al. Novel nicotinonitrile derivatives bearing imino moieties enhance apoptosis and inhibit tyrosine kinase. *Anticancer Agents Med. Chem.* **18**(11), 1589–1598 (2018).
44. Hashem, A. I., Abou-Elmagd, W. S. I., El-Bordany, E. A. & Abdel Aziz, A. Synthesis and reactions of a 2 (5 H)-furanone bearing two furyl substituents. *J. Heterocycl. Chem.* **56**(1), 218–225 (2019).
45. Xu, F. et al. Solvent-free synthesis of 2-aminothiophene-3-carbonitrile derivatives using high-speed vibration milling. *J. Chem. Res.* **38**(7), 450–452 (2014).
46. Azab, M. E. Utility of the enamionitrile moiety in the synthesis of some biologically active thienopyrimidine derivatives. *Phosphorus Sulfur Silicon Relat. Elements* **183**(7), 1766–1782 (2008).
47. Shalaby, M. A., Fahim, A. M. & Rizk, S. A. Antioxidant activity of novel nitrogen scaffold with docking investigation and correlation of DFT stimulation. *RSC Adv.* **13**(21), 14580–14593 (2023).
48. Ali, S. A. et al. Design, synthesis, molecular modelling and biological evaluation of novel 3-(2-naphthyl)-1-phenyl-1H-pyrazole derivatives as potent antioxidants and 15-Lipoxygenase inhibitors. *J. Enzyme Inhib. Med. Chem.* **35**(1), 847–863 (2020).
49. Gouda, M. A. S., Salem, M. A. I. & Mahmoud, N. F. H. 3D-pharmacophore study molecular docking and synthesis of pyrido [2, 3-d] pyrimidine-4 (1 H) dione derivatives with in vitro potential anticancer and antioxidant activities. *J. Heterocycl. Chem.* **57**, 3988–4006 (2020).
50. Barreca, M., Qin, Y., Cadot, M. E. H., Barraja, P. & Bach, A. Advances in developing noncovalent small molecules targeting Keap1. *Drug Discov. Today* **28**(12), 103800 (2023).
51. Li, M. et al. Discovery of Keap1–Nrf2 small-molecule inhibitors from phytochemicals based on molecular docking. *Food Chem. Toxicol.* **133**, 110758 (2019).
52. Chalkha, M. et al. Crystal structure, Hirshfeld surface and DFT computations, along with molecular docking investigations of a new pyrazole as a tyrosine kinase inhibitor. *J. Mol. Struct.* **1273**, 134255 (2022).
53. Geerlings, P., DeProft, F. & Langenaeker, W. Conceptual density functional theory. *Chem. Rev.* **103**, 1793–1874 (2003).
54. Chattaraj, P. K. *Chemical Reactivity Theory* (CRC Press, 2009).
55. Dennington, R., Keith, T.A. and Millam, J.M. GaussView 6.0. 16. Semichem Inc.: Shawnee Mission, KS, USA, pp.143–150, (2016).
56. Frisch, M.J., 2016. Gaussian 16/Gaussian (2016).
57. Liu, C. et al. Computational network biology: data, models, and applications. *Phys. Rep.* **846**, 1–66 (2019).
58. Parr, R. G. & Yang, W. *Density Functional Theory of Atoms and Molecules* (Oxford University Press, 1989).
59. Parr, R. G. & Yang, W. Density-functional theory of the electronic structure of molecules. *Annu. Rev. Phys. Chem.* **46**, 701–728 (1995).
60. Parr, R. G. & Yang, W. T. Density functional approach to the frontier-electron theory of chemical reactivity. *J. Am. Chem. Soc.* **106**, 4049–4050 (1984).
61. Ayers, P. W., Yang, W. & Bartolotti, L. J. Fukui Function. In *Chemical Reactivity Theory* (ed. Chattaraj, P. K.) 255–267 (CRC Press, 2009).

62. Morell, C., Grand, A., Gutiérrez-Oliva, S. & Toro-Labbé, A. Using the reactivity selectivity descriptor $Df(r)$ in organic chemistry. In *Theoretical Aspects of Chemical Reactivity* (ed. Toro-Labbé, A.) 101–117 (Elsevier, 2007).
63. Fuentealba, P., Florez, E. & Tiznado, W. Topological analysis of the Fukui function. *J. Chem. Theory Comput.* **2010**(6), 1470–1478 (2010).
64. Pilepic, V. & Uršic, S. Nucleophilic reactivity of the nitroso group. Fukui function DFT calculations for nitroso benzene and 2-methyl-2-nitrosopropane. *J. Mol. Struct. Theochem.* **538**, 41–49 (2001).
65. Petersson, W. G. & Al-Laham, A. A complete basis set model chemistry. II. Open-shell systems and the total energies of the first-row atoms. *J. Chem. Phys.* **94**, 6081–6090 (1991).
66. Ghareeb, M. A. et al. HPLC-DAD-ESI-MS/MS analysis of fruits from Firmiana simplex (L.) and evaluation of their antioxidant and antigenotoxic properties. *J. Pharm. Pharmacol.* **70**, 133–142 (2018).
67. Ghareeb, M. et al. HPLC-ESI-MS/MS profiling of polyphenolics of a leaf extract from Alpinia zerumbet (Zingiberaceae) and its anti-inflammatory, anti-nociceptive, and antipyretic activities in vivo. *Molecules* **23**(12), 3238 (2018).
68. Ghareeb, M., Saad, A., Ahmed, W., Refahy, L. & Nasr, S. HPLC-DAD-ESI-MS/MS characterization of bioactive secondary metabolites from Strelitzia nicolai leaf extracts and their antioxidant and anticancer activities in vitro. *Pharmacogn. Res.* **10**, 368 (2018).
69. Prieto, P., Pineda, M. & Aguilar, M. Spectrophotometric quantitation of antioxidant capacity through the formation of a phosphomolybdenum complex: specific application to the determination of vitamin E. *Biochem.* **269**, 337–341 (1999).
70. Sobeh, M. et al. Tannin-rich extract from *lannea stuhlmannii* and *lannea humilis* (Anacardiaceae) exhibit hepatoprotective activities *in vivo* via enhancement of the anti-apoptotic protein Bcl-2. *Sci. Rep.* **8**, 9343 (2018).
71. Adeboye, O. Computational modelling procedures for geometry optimization, kinetic and thermodynamic calculations using spartan software: A review. *Arc. Org. Inorg. Chem. Sci.* **1**, 122–125 (2018).
72. Ezz Eldin, R. R. et al. Ligand-based design and synthesis of N'-Benzylidene-3, 4-dimethoxybenzohydrazide derivatives as potential antimicrobial agents; evaluation by in vitro, in vivo, and in silico approaches with SAR studies. *J. Enzyme Inhib. Med. Chem.* **37**(1), 1098–1119 (2022).
73. Hammoud, M. M. et al. Design, synthesis, biological evaluation, and SAR studies of novel cyclopentaquinoline derivatives as DNA intercalators, topoisomerase II inhibitors, and apoptotic inducers. *J. Chem.* **46**(23), 11422–11436 (2022).
74. Yuan, S., Chan, H. S. & Hu, Z. Using PyMOL as a platform for computational drug design. *Wiley Interdiscipl. Rev. Comput. Mol. Sci.* **7**(2), 1298 (2017).
75. A. Frisch, *gaussian 09W Reference*. Wallingford, USA, 25p 470 (2009).
76. Abbass, E. M., Khalil, A. K., Abdel-Mottaleb, Y. & Abdel-Mottaleb, M. S. Exploiting modeling studies for evaluating the potential antiviral activities of some clinically approved drugs and herbal materials against SARS-CoV-2: Theoretical studies toward hindering the virus and blocking the human cellular receptor. *Polycycl. Aromat. Compd.* **44**, 1–12 (2023).
77. Al-Muntaser, S. M. et al. Novel 4-thiophenyl-pyrazole, pyridine, and pyrimidine derivatives as potential antitumor candidates targeting both EGFR and VEGFR-2; design, synthesis, biological evaluations, and in silico studies. *RSC adv.* **13**(18), 12184–12203 (2023).
78. Koopmans, T. Über die Zuordnung von Wellenfunktionen und Eigenwerten zu den einzelnen Elektronen eines Atoms. *Physica* **1**(1–6), 104–113 (1934).

Acknowledgements

The authors thank Mustafa A. S. Gouda (mustafagouda@sci.asu.edu.eg) Chemistry department, faculty of science, Ain Shams University, Cairo, Egypt For his great efforts in computational study (Molecular docking and DFT calculations)

Author contributions

M.G. Methodology, writing the original draft, validation, data curation and A.H. supervision and E.A. supervision, validation, data curation and A.E. supervision and N.F. Methodology, editing the manuscript, validation, data curation.

Declarations

Competing interests

The authors declare no competing interests.

Additional information

Supplementary Information The online version contains supplementary material available at <https://doi.org/10.1038/s41598-024-74275-x>.

Correspondence and requests for materials should be addressed to M.G.B.

Reprints and permissions information is available at www.nature.com/reprints.

Publisher's note Springer Nature remains neutral with regard to jurisdictional claims in published maps and institutional affiliations.

Open Access This article is licensed under a Creative Commons Attribution-NonCommercial-NoDerivatives 4.0 International License, which permits any non-commercial use, sharing, distribution and reproduction in any medium or format, as long as you give appropriate credit to the original author(s) and the source, provide a link to the Creative Commons licence, and indicate if you modified the licensed material. You do not have permission under this licence to share adapted material derived from this article or parts of it. The images or other third party material in this article are included in the article's Creative Commons licence, unless indicated otherwise in a credit line to the material. If material is not included in the article's Creative Commons licence and your intended use is not permitted by statutory regulation or exceeds the permitted use, you will need to obtain permission directly from the copyright holder. To view a copy of this licence, visit <http://creativecommons.org/licenses/by-nc-nd/4.0/>.

© The Author(s) 2024